



HAL
open science

Intra-skeletal calcite in a live-collected *Porites* sp.: Impact on environmental proxies and potential formation process

Claire E. Lazareth, Caroline Soares-Pereira, Eric Douville, Chloé Brahmi,
Delphine Dissard, Florence Le Cornec, François Thil, Cécile
Gonzalez-Roubaud, Sandrine Caquineau, Guy Cabioch

► To cite this version:

Claire E. Lazareth, Caroline Soares-Pereira, Eric Douville, Chloé Brahmi, Delphine Dissard, et al.. Intra-skeletal calcite in a live-collected *Porites* sp.: Impact on environmental proxies and potential formation process. *Geochimica et Cosmochimica Acta Supplement*, 2016, 176, pp.279-294. 10.1016/j.gca.2015.12.020 . hal-01253864

HAL Id: hal-01253864

<https://hal.sorbonne-universite.fr/hal-01253864v1>

Submitted on 11 Jan 2016

HAL is a multi-disciplinary open access archive for the deposit and dissemination of scientific research documents, whether they are published or not. The documents may come from teaching and research institutions in France or abroad, or from public or private research centers.

L'archive ouverte pluridisciplinaire **HAL**, est destinée au dépôt et à la diffusion de documents scientifiques de niveau recherche, publiés ou non, émanant des établissements d'enseignement et de recherche français ou étrangers, des laboratoires publics ou privés.

Accepted Manuscript

Intra-skeletal calcite in a live-collected *Porites* sp.: Impact on environmental proxies and potential formation process

Claire E. Lazareth, Caroline Soares-Pereira, Eric Douville, Chloé Brahmi, Delphine Dissard, Florence Le Cornec, François Thil, Cécile Gonzalez-Roubaud, Sandrine Caquineau, Guy Cabioch

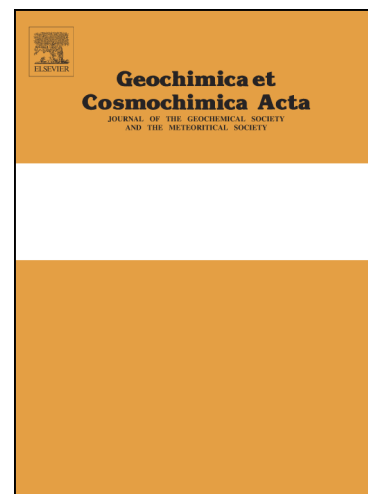
PII: S0016-7037(15)00714-0
DOI: <http://dx.doi.org/10.1016/j.gca.2015.12.020>
Reference: GCA 9552

To appear in: *Geochimica et Cosmochimica Acta*

Received Date: 12 March 2015
Accepted Date: 17 December 2015

Please cite this article as: Lazareth, C.E., Soares-Pereira, C., Douville, E., Brahmi, C., Dissard, D., Cornec, F.L., Thil, F., Gonzalez-Roubaud, C., Caquineau, S., Cabioch, G., Intra-skeletal calcite in a live-collected *Porites* sp.: Impact on environmental proxies and potential formation process, *Geochimica et Cosmochimica Acta* (2015), doi: <http://dx.doi.org/10.1016/j.gca.2015.12.020>

This is a PDF file of an unedited manuscript that has been accepted for publication. As a service to our customers we are providing this early version of the manuscript. The manuscript will undergo copyediting, typesetting, and review of the resulting proof before it is published in its final form. Please note that during the production process errors may be discovered which could affect the content, and all legal disclaimers that apply to the journal pertain.



Intra-skeletal calcite in a live-collected *Porites* sp.: Impact on environmental proxies and potential formation process

Claire E. Lazareth^{1,*}, Caroline Soares-Pereira¹, Eric Douville², Chloé Brahmi³, Delphine Dissard¹, Florence Le Cornec¹, François Thié², Cécile Gonzalez-Roubaud², Sandrine Caquineau¹, Guy Cabioch^{1,†}

¹IRD-Sorbonne Universités (UPMC, Univ. Paris 06)-CNRS-MNHN, LOCEAN Laboratory, IRD France-Nord, 32, avenue Henri Varagnat, F-93143 Bondy, France

²Laboratoire des Sciences du Climat et de l'Environnement (LSCE/IPSL, UMR 8212 CNRS-CEA-UVSQ), 91198 Gif-sur-Yvette Cedex, France

³Université de la Polynésie française- UMR 241 EIO - BP 6570 - 98 702 Faa'a – Tahiti

† Deceased

* Corresponding author: Tel.: + 33 1 48 02 59 64; fax: + 33 1 48 02 55 54.

E-mail address: claire.lazareth@ird.fr (C.E. Lazareth)

Keywords: Tropical corals, Diagenesis, Calcite, Aragonite, Geochemical Proxies

Abstract

Geochemical proxies measured in the carbonate skeleton of tropical coral *Porites* sp. have commonly been used to reconstruct sea surface temperature (SST) and more recently seawater pH. Nevertheless, both reconstructed SST and pH depend on the preservation state of the skeleton, here made of aragonite; i.e., diagenetic processes and its related effects should be

limited. In this study, we report on the impact of the presence of intra-skeletal calcite on the skeleton geochemistry of a live-collected *Porites* sp..The *Porites* skeleton preservation state was analyzed using X-ray diffraction and scanning electron microscopy. Sr/Ca, Mg/Ca, U/Ca, Ba/Ca, Li/Mg, and B/Ca ratios were measured at a monthly and yearly resolution using solution ICP-MS and multi-collector ICP-MS. The $\delta^{11}\text{B}$ signatures and the calcite percentages were acquired at a yearly timescale. The coral colony presents two parts, one with less than 3% calcite (referred to as "no-calcite" skeleton), the other one, corresponding to the skeleton formed during the last 4 yrs. of growth,with calcite percentages varying from 13 to 32% (referred to as "with calcite" skeleton). This intra-skeletal calcite replaces partly or completely numerouscenter of calcification (COCs). All geochemical tracers investigated are significantlyimpacted by the presence of calcite. Thereconstructed SSTdecreasesby about0.1°C per calcite-percent as inferred fromthe Sr/Ca ratio. Such impact reaches up to 0.26°C per calcite-percent for temperature deduced from the Li/Mg ratio. So, less than 5% of such intra-skeletal calcite does not prevent SST reconstructions using Sr/Ca ratio, but the percentage and type of calcite have to be determined before fine SST interpretation. Seawater pH reconstruction inferredfrom boron isotopes drop by about -0.011 pH-unit per calcite-percent. Such sensitivity to calcite presence is particularly dramatic for fine paleo-pH reconstructions. Here we suggest that after being brought to shallow waters following a cyclone, the studied coral was seasonally subjected to rainfall-related water freshening that could have mimicked a vadose environment like can be encountered on raised fossil coral reefs. Nevertheless, the process of calcite precipitation remains to be determined.

1. Introduction

To better understand global change, e.g., distinguish natural vs. anthropic effects on climate, and decrease uncertainties in climate model simulations, reconstructions of past SST and pH at decadal and inter-annual resolution occupy a large scientific community. In tropical settings, acquisition of paleo-SST are currently obtained using $\delta^{18}\text{O}$ and/or trace elements from aragonite skeleton of scleractinian corals, mostly *Porites* sp. (e.g., Alibert and McCulloch, 1997; Beck et al., 1992; Corrège, 2006; Liu et al., 2009; Wu et al., 2013). In the massive coral *Porites* sp., the Sr/Ca ratio is the most commonly used proxy for SST reconstructions (e.g., Corrège, 2006; Gagan et al., 1998; Zinke et al., 2014). This proxy, however, depends on the coral location and species; for instance more than 16 paleo-SST equations based on the Sr/Ca ratio exist for Indo-Pacific *Porites* sp. (Corrège, 2006; Gagan et al., 2000). Variation of the Sr/Ca-SST dependency limits the proxy accuracy and therewith its utility, particularly in regions where seasonal temperature changes are limited. Recently, the Li/Mg ratio in aragonite scleractinian coral skeleton has been shown to be a species independent SST proxy that could complement previous temperature proxy (Case et al., 2010; Hathorne et al., 2013a; Montagna et al., 2014). To reconstruct the pH of the seawater, the U/Ca ratio in tropical corals was proposed (Inoue et al., 2011) but its strong sensitivity to temperature clearly limits paleo-pH applications. Contrarily, boron isotopes in *Porites* sp. skeleton has been used with success to reconstruct paleo-pH of surface seawater and ocean acidification related to the inception and development of the industrial era (e.g., Douville et al., 2010; Liu et al., 2009; Shinjo et al., 2013a; Wei et al., 2009; Wu et al., 2013). Even if boron isotopes in corals are now considered to be directly the reflect of pH of the calcification fluid (Allison et al., 2010; Blamart et al., 2007; Rollion-Bard et al., 2003; Venn et al., 2011), Trotter et al. (2011) highlighted that pH of the calcification in scleractinian corals depends on pH of seawater. In

addition, experimental cultures of tropical corals such as genus *Porites* or *Acropora* at various seawater pH revealed empirical pH- $\delta^{11}\text{B}$ calibration curves (Hönisch et al., 2004; Reynaud et al., 2004).

Independently of the accuracy of the above-described proxies, the reliability of paleoclimate reconstructions also depends on the coral skeleton preservation (or diagenesis) state. Skeleton alterations (e.g., dissolution, mineralogical change) and secondary precipitations in the skeleton pores (e.g., calcite, aragonite, brucite) or in microboring galleries (filled by calcite), both in live-collected or fossil corals, can indeed affect the coral geochemical signature, which then does not reflect pristine forcing anymore. The impacts of diagenesis on the coral skeleton geochemistry have been investigated in several studies (e.g., Allison et al., 2007; Bar-Matthews et al., 1993; Houk et al., 1975; Lazareth et al., 2013; Nothdurft and Webb, 2009). Nevertheless, the impacts of some specific diagenesis on the skeleton's geochemistry are poorly known. This is the case for intra-skeletal calcite, such as described by Rabier et al. (2008) and McGregor and Gagan (2003) for example. Moreover, although the impacts of diagenesis have been studied for almost each proxy independently, only very few studies report on multi-proxy approach allowing for a more global picture of a specific archive (Allison et al., 2007; Griffiths et al., 2013; Hendy et al., 2007). Lastly, the impacts of diagenesis on the recently validated Li/Mg and $\delta^{11}\text{B}$ proxies are poorly documented.

In this study, we investigated the impact of intra-skeletal calcite on trace elements concentration and boron isotope composition in a modern, live-collected, *Porites* sp. coral. A possible origin of the intra-skeletal calcite is proposed.

2. Material and methods

2.1. Sample location and preparation

A living colony of *Porites sp.* was collected in September 2009 in the Mapuna Bay on the east coast of the Epi Island, Vanuatu (16°35'S - 168°12'E; Fig. 1). The colony (50 cm in diameter and 20 cm height) was collected in less than 3 m water depth, rinsed with freshwater and carefully dried. A 1 cm-thick slab along the maximum growth axis was then sampled, rinsed in deionized water in an ultrasonic bath, and dried overnight. An X-ray radiography of the slab was taken to identify the density bands and determine the growth axis along which the geochemical analyses were conducted.

2.2. Methodologies for diagenesis characterization

The percentages of aragonite vs. calcite were determined on powdered skeleton fragments collected in recent and oldest parts of the colony by X-ray diffraction analysis using a Siemens D500 diffractometer (Ni-filtered CuK α radiation) operating at 40 kV and 30 mA with 8s counting every 0.02°. Semi-quantitative estimations of aragonite and calcite mass percentage were done using calibration curves established from known concentrations of aragonite and calcite. Average error made on the calcite percentage measurement is 7% (2 σ). Seven additional XRD analyses were conducted on powder left over from boron isotopic analyses (see & 2.3.).

Five coral fragments (~ 1 to 2 cm²) were sampled from the recent (living) to the oldest part of the coral colony and prepared for scanning electron microscopy (SEM) observations. The fragments were manually broken, cleaned, and dried before being sputter-coated using platinum. Observations were done using a Zeiss EVO[®]-LS15 SEM.

2.3. Geochemical analyses using ICP-MS and MC-ICP-MS

A micro-sampling system was used to collect ~1 mg-powders for trace element analyses. 132 samples were collected along a line parallel to the growth axis, with a step size of 0.8 mm (Fig. 2) allowing for a monthly resolution.

The coral powders were dissolved in 2 wt% nitric acid. Three internal standards were added in every solution, Scandium (Sc), Yttrium (Y), and Indium (In) at a concentration of 50 $\mu\text{g.l}^{-1}$ for Sc and Y and 5 $\mu\text{g.l}^{-1}$ for In. Element concentrations were then measured using an Inductively Coupled Plasma Mass Spectrometer (ICP-MS; Agilent 7500cx®). The precision of measurements was determined using the standard deviations (1σ) calculated on repeated analyses of several aliquots of a home-made coral standard. The chemical elements chosen were Sr, U, Mg, Li, B and Ca. The precision was 0.07 mmol/mol for Sr/Ca, 0.02 mmol/mol for Mg/Ca, 0.01 $\mu\text{mol/mol}$ for U/Ca, 0.25 $\mu\text{mol/mol}$ for Li/Ca and 2 $\mu\text{mol/mol}$ for B/Ca. The accuracy was assessed against the external certified *Porites* sp. GSJ standard JCp-1 (Hathorne et al., 2013b). Profiles were anchored in time using the AnalySeries software (Paillard et al., 1996). The anchoring points were the collection date (i.e., September 2009) and the winter Sr/Ca ratio data, i.e., the Sr/Ca ratio maxima.

To quantify the impact of the presence of calcite on elemental ratios and to determine the isotopic composition of boron ($\delta^{11}\text{B}$), at a yearly timescale approximately, seven large samples were collected parallel to the high-resolution profile (Fig. 2). In that aim, the banding pattern was used to determine the size of each "yearly" sample. Each 1-gram size sample was crushed before aliquot sampling. Trace element ratios were measured using an ICP-QMS Xseries^{II} Thermo Scientific® following the analytical protocol developed at the LSCE in Gif/Yvette, France (Bourdin et al., 2011; Hathorne et al., 2013b). The measurements of boron isotopes were also performed at the Laboratoire des Sciences du Climat et de l'Environnement (LSCE) using a multi-collector ICP-MS Neptune^{Plus} Thermo Scientific®. To test the

reproducibility of the boron isotope analysis at various sizes, samples were systematically prepared twice, using 200 mg and 50 mg of material. The LSCE's batch protocol was used to purify and extract boron in final 0.1 N nitric acid solutions as previously described (Dissard et al., 2012; Douville et al., 2010). The 200 ppb-B solutions were introduced into the mass spectrometer through a PFA-50 μ L/min nebulizer and a micro-cyclonic chamber, limiting the blank contribution below 0.5%. The $\delta^{11}\text{B}$ values were determined using the bracketing protocol with standard NIST NBS-951 (0‰) with an analytical uncertainty of 0.25‰ (2σ). The $\delta^{11}\text{B}$ values obtained for the reference materials boric acid NBS-951, giant clam JCt-1, *Porites* coral JCp-1, and open ocean seawater NASS-II included in the treatment batch were 0.07, 16.17, 24.25 and 39.63‰ respectively. Such values are in agreement with a recent study on seawater with a value of 39.61‰ (Foster et al., 2010) or with results issued from a recent inter-lab calibration exercise on biocarbonate materials JCp-1 and JCt-1 with mean values at around 24.3 ‰ and 16.3 ‰ respectively (Gutjahr et al., 2014). The size of the material sampled does not impact the $\delta^{11}\text{B}$ results as all obtained results are inside analytical uncertainties and, consequently, the pH values were calculated using the average of the $\delta^{11}\text{B}$ values for 200 mg and 50 mg for each of the seven coral blocks. The $\delta^{11}\text{B}$ results were anchored in time by attributing a date, based on the Sr/Ca geochemical profile, to the middle of each sampled block. Strontium isotopes ($^{87}\text{Sr}/^{86}\text{Sr}$ ratio) were measured with the remaining of the seven annual *Porites* powders studied here. The measurements were performed at the LSCE, on the same MC-ICP-MS Neptune^{Plus} as for $\delta^{11}\text{B}$, using the analytical protocol previously described by Palmiotto et al. (2013).

2.4. Sea surface temperature reconstruction

To calculate SST based on Sr/Ca ratio, we used the bimonthly-resolved Sr/Ca-SST relationship established from a *Porites* sp. from the Fiji island (Wu et al., 2013) because this island is close to the Vanuatu and shares similar environmental conditions. The SST reconstruction based on Li/Mg ratio was obtained using the equation established by Montagna et al. (2014). Reconstructed SSTs were compared to IGOSS monthly SST data (referred as "gridded-SST" in this manuscript) for the grid cell 168.5E-16.5S (Reyn_SmithOiv2¹; Reynolds et al., 2002).

2.5. pH reconstruction

Empirical relationships between $\delta^{11}\text{B}$ and pH_{sw} were determined by Hönisch and Hemming (2004) and Reynaud et al. (2004) for cultured tropical corals (*Porites*, *Acropora*) at various pH conditions. Based on these studies and the unique empirical calibration proposed in 2007 for various biogenic carbonates by Hönisch et al. (2007), seawater pH (pH_{sw}) was calculated using an empirical factor of isotopic fractionation (α) of about 1.020 with no further species-specific "vital effect" correction for *Porites* (Hönisch et al., 2007). Depending on the used calibration curve existing in the literature, the α value which has to be considered is still debated making qualitative pH_{sw} assessments more difficult. As a result, we chose here to focus our observations mainly on pH_{sw} differences between the "with calcite" and "no calcite" skeleton. The other parameters used are a seawater $\delta^{11}\text{B}$ value of 39.61‰ (Foster et al., 2010) and a pK_{B} value of 8.56 (Dickson, 1990) corresponding to average temperature and salinity values of 27.9°C and 34.88, respectively. Reconstructed pH uncertainties are less than ± 0.08 including analytical uncertainties and annual changes of temperature ($\pm 0.5^\circ\text{C}$) or salinity

¹ Available at http://iridl.ldeo.columbia.edu/SOURCES/.IGOSS/.nmc/.Reyn_SmithOiv2/.monthly/.sst/

(± 0.2). Such uncertainties are clearly low compared to the amplitude of pH change determined in our study (i.e., about 0.4 pH-unit).

3. Results

The *Porites* sp. colony collected alive in September 2009 presents a distinct dark line 8 cm away from the living growth surface. On the X-Ray, this line clearly divides the colony in two parts. Below this line, the skeleton is characterized by a fine banding pattern, obscuring the usual annual growth bands and contrasting to what is observed above the line (Fig. 2). In addition, an interruption of the growth can be seen on the left side of the colony, with a recovery leading to a curved extension of the colony afterwards (like a bump on the left). Consequently, the geochemical analyses were conducted in the middle of the right part of the colony where the growth seems continuous. Five years are counted from the top of the colony to the dark line that would thus correspond to the beginning of year 2004.

3.1. Diagenesis features: quantification and distribution of calcite in the coral skeleton

The percentage of calcite in the coral colony ranges from 0 to $32 \pm 7\%$. Before the year 2004, i.e., below the dark line described above, calcite percentages are less than 2%. After 2004, toward the living part of the colony and along the geochemical profile, the calcite percentage is 3% in the first centimeter, then it increases to reach a maximum of 32% before decreasing. Close to the top of the colony, the calcite percentage is still high, i.e., 13% (Fig. 2). In this study, we choose to divide the coral in two parts, considering the XRD results done along the geochemical sampling line: i) the part containing a maximum of 3.4% of calcite (average of 1.3%) and ii) the part containing more than 8% of calcite (average of 24%). For convenience,

the part with less than 3% will be termed the “no-calcite” skeleton and the one with more than 8% the “with-calcite” skeleton.

In the “no-calcite” part, the skeleton is very well preserved, with inter-skeletal pore spaces free of any deposit or secondary crystallization (Fig. 3a) and without dissolution features (Fig. 3b-d). Empty microborer galleries are observed (Fig. 3b-c). The “with-calcite” skeleton also has no cement in the pore spaces and aragonite fibers are well preserved (Fig. 4a). In some restricted areas, some secondary aragonite is observed located in the pore spaces (not shown). Some, but not all, microborer galleries are filled with calcite (Fig. 4b). Otherwise, calcite strictly occurs inside the coral skeletal structures (and not in the pore spaces between skeletal elements) and was observed even in the upper 5 mm corresponding to the “living-part” of the colony (i.e., tissue-covered skeleton part). Calcite occurs as flat, homogeneous, and compact-like areas (Fig. 4). Except the few microborer galleries mentioned above, the calcite is exclusively located in the centers of calcification (COCs), either as line-patches (Fig. 4c) or completely replacing the COCs (Fig. 4d-e). The contact between the calcite and the surrounding aragonite fibers is neat (Fig. 4e&h). When the COCs are not completely replaced by calcite, their specific microstructure (i.e., granular appearance of aragonite crystals) is still visible between the calcite and the aragonite fibers, with a neat contact between both ultrastructural components (i.e., no sign of dissolution) (Fig. 4g).

3.2. Geochemical signature of pristine coral aragonite vs. calcite-containing skeleton

The geochemical profiles obtained cover 8 years of coral growth, from 2001 to 2009 (recovery date; data in Suppl. Mat., Table 1). All profiles are presented with a y-axis orientation corresponding to the element/SST relationship when relevant, i.e., inverted for Sr/Ca, B/Ca, U/Ca, and Li/Mg (Fig. 5). High resolution profiles of Sr/Ca and U/Ca exhibit a

marked seasonal pattern. A seasonal pattern is also observed for Mg/Ca, Li/Mg, and B/Ca but appears less pronounced. Annual growth rate was calculated using winter peak's distances from the Sr/Ca profile. No significant difference is found between growth rates (skeletal extension rates) of the two skeleton parts (t-test) with a global average growth rate of $13.3 \pm 2.1 \text{ mm.yr}^{-1}$. All profiles can be split in two, corresponding to the “no-calcite” vs. “with-calcite” skeleton parts. Indeed, there is a quite clear compositional shift when reaching the colony part containing 21% of calcite (corresponding to the beginning of the year 2005; Fig. 5). For Sr/Ca, the summer values are all lower in the “with-calcite” than in the “no-calcite” skeleton. The first two winter Sr/Ca values stay close to the “no-calcite” ones (around 9.2 mmol/mol), then a value as low as 8.9 mmol/mol is observed (represented by a star on Fig. 5a; corresponding to winter 2007-2008) before increasing to ~ 9.1 mmol/mol. For U/Ca, a slight decrease is observed in the summer values of the “with-calcite” skeleton while the winter ones are more varied. For Li/Mg and B/Ca ratios, a global decrease is observed while an increase can be seen for the Mg/Ca ratio. Considering the point on the geochemical profile corresponding to the shift between 3 and 21% of calcite, element/Ca ratio mean values were calculated for the “no-calcite” and “with-calcite” skeleton (Fig. 5). All the mean element/Ca ratios of the “no-calcite” are significantly different compared to the mean of the “with-calcite” skeleton (t-test, $p < 0.05$). The same results were obtained at the yearly timescale (Fig. 5).

The $\delta^{11}\text{B}$ values range from 20.92 to 23.26‰ and the yearly-B/Ca ratios vary from 0.26 to 0.43 mmol/mol. The mean $\delta^{11}\text{B}$ and yearly-B/Ca values obtained are 23.14‰ and 0.44 mmol/mol and 21.78‰ and 0.33 mmol/mol for the “no-calcite” and the “with-calcite” skeleton respectively (Fig. 5). The $\delta^{11}\text{B}$ and the resulting calculated pH_{sw} are proportionally impacted by the presence of calcite (Fig. 6).

The strontium isotope values showed invariable and modern marine signature (0.709165 ± 0.000012 , 2σ , $n = 7$).

3.3. Impact of intra-skeletal calcite on SST and pH reconstructions

Gridded-SST between 2001 and 2010 vary between 25.6 and 29.9°C with a mean at $27.9 \pm 1.2^\circ\text{C}$ (1σ) (Reynolds et al., 2002). Satellite SSTs remain similar before and after 2005 (ANOVA test). To compare reconstructed SST to gridded-SST, reconstructed SST based on Sr/Ca and Li/Mg coral ratios was split in two datasets, corresponding to the “no-calcite” (before 2005) and “with-calcite” (after 2005) skeleton, and averaged. For the “no-calcite” skeleton, no significant difference is found between the mean reconstructed and gridded-SSTs (t-test, $p > 0.3$), with 0.2 and 1.3% of average difference for reconstructed-SST vs. gridded-SST using Sr/Ca and Li/Mg ratios. For the “with calcite” skeleton (average of 24% calcite), reconstructed SST are significantly higher than the gridded-SSTs (t-test, $p = 0$). Indeed, using Sr/Ca and Li/Mg ratios, the reconstructed SSTs present an average shift of $+3.3^\circ\text{C}$ (12%) and $+4.2^\circ\text{C}$ (13.6%) respectively (Fig. 7). The highest difference observed is $+5.9^\circ\text{C}$ with Sr/Ca and $+7.8^\circ\text{C}$ with Li/Mg (summer 2007-08). Lastly, the reconstructed SSTs for the “no-calcite” skeleton are similar using Sr/Ca or Li/Mg (t-test, $p > 0.4$) whereas a difference exists for the “with-calcite” skeleton, i.e., Li/Mg reconstructed-SST being more impacted than Sr/Ca reconstructed-SST (t-test, $p < 0.05$; Fig. 7b).

Using a main annual SST of $27.9 \pm 0.3^\circ\text{C}$ and a salinity of 34.9 ± 0.2 , pH_{sw} values (as calculated from $\delta^{11}\text{B}$) ranged between 7.53 ± 0.08 and 7.96 ± 0.04 .

4. Discussion

4.1 Origin of the intra-skeletal calcite: Biogenic vs. early diagenesis

Considering the “ $\delta^{11}\text{B}$ -calcite ‰” linear correlation (Fig. 6) we calculated a value of $17.05 \pm 0.85\text{‰}$ for a virtual 100%-calcite end-member with a constant seawater $\delta^{11}\text{B}$ value of 39.61‰ (Foster et al., 2010). This would correspond to a calculated $\text{pH}_{\text{solution}}$ of about 7.87 ± 0.11 . It can be noted that such low $\delta^{11}\text{B}$ value was recently observed for calcite cold-water octocorals (Farmer et al., 2015; McCulloch et al., 2012) which calcifying fluid pH falling within 7.6-8.0. Nevertheless, in a biologically-controlled biomineralization, aragonite and calcite precipitation strictly results from the control of the organic matrix compounds, in the scleractinian coral case synthesized by the calcicoblastic epithelium (Falini et al., 1996; Falini et al., 2013; Mass et al., 2013; Puvarel et al., 2005; Rahman et al., 2011; Tambutté et al., 2011). To date, no coral species has been found to produce both CaCO_3 polymorphs in natural modern seawater conditions, even in the primary skeleton formed by coral post-larvae (Clode et al., 2011). In addition, the calcite crystals are massive with a flat and homogeneous surface. In other coral diagenesis studies (Frankowiak et al., 2013; McGregor and Gagan, 2003), these characteristics correspond to calcite crystals called calcite spar, most probably of non-biogenic origin (Dalbeck et al., 2011). Moreover, using the relationship between the Sr/Ca signature and the calcite-%, we calculated a 100% calcite Sr/Ca ratio end-member of $\sim 7.96 \pm 0.31$ mmol/mol. This is higher than calcite corals Sr/Ca ratios (below 5 mmol/mol on average; e.g., Sinclair et al., 2011; Thresher et al., 2010) but close to the average value for diagenetic intra-skeletal calcite (Table 1, Rabier et al., 2008, fig. 8). Considering those evidences, the hypothesis of a biogenic origin for the observed intra-skeletal calcite cannot be supported.

Even though few microborer galleries were found calcite-filled, the intra-skeletal calcite observed in our sample occurred as partial or total replacement of COCs. It was shown that the two ultrastructural components of coral skeleton i.e., COC and fibers, are characterized by

different nanostructural organization and geochemical signatures (Benzerara et al., 2011; Cuif and Dauphin, 2005; Meibom et al., 2007; Nothdurft and Webb, 2007; Perrin, 2003; Stolarski and Mazur, 2005). Considering geochemical signatures, Meibom et al. (2007) reported a depletion of Sr/Ca in COCs compared to fibers in *Porites* sp.. In contrast, Allison and Finch (2004) found a higher Sr/Ca ratio in COCs than in fibers for the *Porites lobata* species, which was confirmed by Allison et al. (2005a). Finch and Allison (2003) suggested that the high Sr content of the coral aragonite makes it less thermodynamically stable compared to abiogenic aragonite. This would favor the COC preferential dissolution, as suggested by Allison et al. (2005b). Additionally, COCs are rich in organics that, besides the sub-micronic size of their aragonite crystals, makes them very quickly degradable (Perrin and Smith, 2007a; Perrin and Smith, 2007b). COCs are therefore the first part of the skeleton to be dissolved (Ayling et al., 2006; Gvirtzman et al., 1973; James, 1974; Perrin and Smith, 2007b; Rabier et al., 2008). In our study, some of the COCs are replaced by calcite and this intra-skeletal calcite was also observed in the first 5 mm of the colony that corresponds to the living tissue part. These observations indicate a very early diagenesis that may have occurred during the last 5 years of life of the coral colony, most probably as soon as the skeleton was deposited. The presence of similar intra-skeletal calcite in a live-collected *Porites lobata* coral was reported by Houk et al. (1975). The authors suggested that the intra-skeletal calcite had a biogenic origin, but such an explanation seems highly improbable as discussed above. In addition, both the habitus of the calcite described by Houk et al. (1975; "clean, blocky, rather angular crystals possessing no internal structure") and its geochemical composition are in favor of a diagenesis-related intra-skeletal calcite.

In studies of subaerial carbonate diagenesis, the replacement of aragonite by calcite without pore cementation (at least in the first steps of diagenesis) is characteristic of the

freshwater vadose and phreatic zone²(James, 1974; Longman, 1980; Pingitore, 1976; Sorauf, 1980). Two main processes for the aragonite-calcite transformation, via dissolution/precipitation, in such environments were proposed. In the vadose zone, the zone of dissolution/precipitation has a width of a 1 μm (or less) where an immobile water film, termed "thin film" or "messenger film", is present (Pingitore, 1976; Rabier et al., 2008). The dissolution/precipitation process in this case occurs in a closed or semi-closed system and precipitation is concomitant to dissolution (James, 1974; Pingitore, 1976; Rabier et al., 2008). In the phreatic zone, the calcite formation occurs via a zone of chalky aragonite of several millimeters wide (James, 1974; Pingitore, 1976). In this case, the calcitization process occurs in an open system. In our study, no chalky zone was observed; the calcite crystals are in neat contact either with the remaining unaltered COC part or with the surrounding aragonite fibers in case of total COC replacement (Fig. 4). This feature closely resembles that which was described for subaerial freshwater vadose diagenesis, as for example in James (1974) (p. 12 and fig. 8d). Because only COCs are (partly) replaced, what we observe might be the very first stage of such subaerial freshwater vadose diagenesis. But in which conditions such a "vadose-like" diagenesis could have occurred in a coral collected alive?

The studied specimen was collected on the Epi Island of the Vanuatu in less than 3 m depth, close to a beach without any riverine freshwater inputs. The absence of such riverine input is confirmed by the $^{87}\text{Sr}/^{86}\text{Sr}$ ratio values indicating a modern marine signature (0.709165 ± 0.000012 , 2σ , $n = 7$). Nevertheless, in such a shallow setting, the coral colony could have been subjected to occasional relative water freshening, related to rainwaters. Precipitations may have acted here in a similar way than freshwater does in subaerial vadose setting. Looking at the reconstructed SST using Sr/Ca, the winter values are similar to the gridded-ones while the

²The vadose zone is comprised between the land and the groundwater surface (also named water table). The freshwater phreatic zone is below the groundwater surface and above the zone where fresh- and marine-water are mixed (e.g., Longman, M.W. (1980) Carbonate diagenetic textures from near surface diagenetic environments. *Am. Assoc. Petrol. Geol. Bulletin* **64**, 461-487.

summer values are higher (Fig. 7a). In Vanuatu, rainfall is more abundant during the summers than during the winters. Consequently, the skeleton accretion during summers would have been more impacted by rainfall-related freshwaters than during winters, resulting in a higher calcite concentration, and thus geochemical modification, during summers.

Concerning the “no-calcite” skeleton part, we hypothesize that environmental conditions were most probably different (e.g., with less freshwater impact) than those encountered during the formation of the “with calcite” skeleton. Considering the location where the coral was collected, this implies a deeper location. In February 2004, the Ivy cyclone passed above Vanuatu. The intensity of this cyclone was at its maximum all along its track above Vanuatu and it skirted the Epi Island at force 4 (i.e., severe tropical cyclone; data from the Australian Government - Bureau of Meteorology³). Such an event could have removed the coral colony from a deeper to a shallower location. Massive coral colony, like *Porites* sp., dislodgment related to cyclones is indeed common (Bries et al., 2004; Cheal et al., 2002; Fabricius et al., 2008; Gilmour and Smith, 2006). What would be in favor of this explanation is the observed change in growth direction of the colony due to a change in the position of the colony. We therefore interpret all the observed features, i.e., partial change in coral growth direction, presence of the skeletal dark line, and appearance of intra-skeletal calcite in the last years of coral growth, as the consequence of a displacement of the colony, related to the Ivy cyclone, from deep to shallow environment where it would then have been more impacted by rainfall than previously. Nevertheless, the difference in living water depth was nevertheless most probably not so important because i) Sr/Ca reconstructed SST before Ivy are similar to satellite data (i.e., surface SST), so the coral was probably not so deep and ii) the growth rate change is limited, as assessed by annual growth calculation from the Sr/Ca signal. Indeed, it was shown that coral living in shallow waters has a higher growth rate than those living in deep

³ <http://www.bom.gov.au/cyclone/history/tracks/index.shtml>

water (e.g., Goreau, 1959; Marubini et al., 2001; Sun et al., 2008). So the limited growth rate change here is in favor of a limited living-depth change. Such limited depth modification also excludes any light-related geochemical change (Juillet-Leclerc et al., 2014).

Nevertheless, we interpret the presence of calcite as being related to occasional water freshening to which the coral colony would have been more exposed after than before the Ivy Cyclone. Geochemical changes in our sample might thus also be related to changes in salinity and in water composition. If such environmental-related geochemical changes can hardly completely be excluded, they are most probably not the main forcing, at least for the Sr/Ca (and most probably Li/Ca) signature, as it was shown that salinity changes and/or freshwater inputs do not impact this tracer (Alibert et al., 2003; Fallon et al., 2003; Moreau et al., 2015). Changes in Ba/Ca, Mn/Ca, U/Ca, and Mg/Ca were observed, but in relation with river flood or runoff (Alibert et al., 2003; Fallon et al., 2003; Sinclair and McCulloch, 2004), which is not applicable in our case. Sr/Ca in seawater, and consequently in the coral skeleton, can be impacted by heavy precipitations in specific settings (Wei et al., 2000). Consequently, even if geochemical modifications related to environmental changes after the coral colony displacement cannot be completely excluded, this phenomenon participates most probably only partially to the observed change.

Still, the question stands about the calcite formation process. Indeed, even in such shallow environment, surrounding water should not be able to pass through the coral tissue to the skeleton as the coral calicoblastic cells composing the mineralizing tissue (in contact with the skeleton) are joined by septate junctions which tightly seal the cell layer (Brahmi et al., 2010; Clode and Marshall, 2002; Tambutté et al., 2007). The presence of intra-skeletal calcite from the living tissue part to 7cm below the living surface cannot be explained by seawater infiltration into the coral skeleton due to i) fish grazing or ii) tissue loss/damages due to the Ivy cyclone because no secondary precipitation was observed in the inter-skeletal pore spaces.

Consequently, at this point, the exact process that led to COC's dissolution and replacement by calcite remains to be determined.

4.2 Intra-skeletal calcite and its impact on reconstructed SST

In the Vanuatu's coral studied, intra-skeletal calcite localized in the centers of calcification is present from the surface of the colony to approximately 7 cm in depth. The presence of this intra-skeletal calcite significantly impacts the geochemical results obtained from the coral skeleton analyses and, thus, the reconstructed environmental variables. When using the Sr/Ca signature of corals for paleo-SST reconstruction, the presence of calcite, which has a lower Sr/Ca ratio than the pristine aragonite, skews reconstructed SST toward higher values than expected (Table 1). To our knowledge, only one study reports on higher Sr/Ca values (lower reconstructed SSTs) for secondary calcite in a fossil coral (Frankowiak et al., 2013). Because the geochemical composition of diagenetic calcite depends on its nature, e.g., cement *vs.* intra-skeletal (Table 1), the range of the SST bias varies as well. Most available data concern calcite cements (in skeleton pores) that display very low Sr/Ca values, leading to an average SST bias of 1 to 1.7°C per calcite-% (e.g., Allison et al., 2007; Griffiths et al., 2013 and Table 1 for other related studies). For a mix of cement and intra-skeletal calcite, McGregor and Gagan (2003) calculated an impact of ~1.15°C per calcite-% and, for calcite meniscus mimicking dissepiments, Dalbeck et al. (2011) calculated a value of +1.2°C per calcite-%. In our case, the calculated SST using seasonal Sr/Ca ratios was, on average, 3.4°C higher than the gridded-SST for a mean of 24% of intra-skeletal calcite. This would correspond to a $+0.14 \pm 0.03$ °C per calcite-% that is confirmed at the yearly timescale with a value of $+0.08 \pm 0.06$ °C per calcite-%. Such impact is lower than those previously reported and the presence of less than 5% of such intra-skeletal calcite (in the COCs) will not prevent SST-reconstruction

based on Sr/Ca ratio; this proxy allowing to reconstruct SST, coarsely, at the near 0.5°C (Beck et al., 1992). Considering the Li/Mg SST proxy, an average $+0.17 \pm 0.04^{\circ}\text{C}$ change per intra-skeletal calcite-% was calculated from our seasonal data. At the yearly scale, this change reaches $0.26 \pm 0.03^{\circ}\text{C}$ per calcite-%. The Li/Mg-deduced temperature is more affected by a small amount of calcite than the Sr/Ca ratio and this impact has to be considered for fine paleo-application using this newly validated temperature proxy.

Looking now at the reconstructed SST in terms of variability, one can note that the SST seasonal cycles are preserved in the “with-calcite” skeleton but with different amplitudes than that of the gridded-SSTones (Fig. 7a). This might reflect an increasing amount of calcite, and potential environmental effects as discussed above, during the summer season. Nevertheless, it is interesting to notice that for the Sr/Ca ratio, the year-to-year relative seasonal amplitude changes are maintained. Indeed, a moderate La Niña (as defined using the Ocean Niño Index) occurred in 2007-2008. In the Vanuatu region, this resulted in a winter with warmer SST than usual (star on Fig. 5a and 7a). This warmer winter is still observable on the Sr/Ca profile, even if located in the skeleton part containing almost 30% of intra-skeletal calcite. Thus, even if up to 30% of intra-skeletal calcite is present in the coral skeleton, the relative seasonal amplitudes are preserved in the Sr/Ca signal and it remains possible to obtain climate-like reliable information such as Niño or Niña year's occurrences.

4.3 Impact on $\delta^{11}\text{B}$, B/Ca, and reconstructed pH

While the $\delta^{11}\text{B}$ and B/Ca ratio values (23.14‰ and 0.44 mmol/mol) obtained for the “no-calcite” skeleton are similar to values published in previous studies for *Porites* sp. (Douville et al., 2010; Hemming et al., 1998; Krief et al., 2010; Pelejero et al., 2005; Shinjo et al., 2013b; Wei et al., 2009), the $\delta^{11}\text{B}$ and B/Ca values obtained for the “with-calcite” skeleton are clearly

low, below 22‰ (Suppl. Mat., Table 2) and 0.35 mmol/mol. In spite of different processes of formation, such low $\delta^{11}\text{B}$ values linked to the non-biogenic calcite presence appear here similar to the ones observed in marine biogenic or inorganic calcite in general. Only a few studies report on boron isotopes in marine biogenic calcite, especially for corals. In brachiopods, Hemming and Hanson (1992) measured $\delta^{11}\text{B}$ values between 20.8 and 23.2‰ while values between 16.8 to 19.6‰ and 14 to 19‰ were obtained more recently (Lécuyer et al., 2002; Penman et al., 2013). Benthic foraminifera calcite present lower $\delta^{11}\text{B}$ (14-17‰), except for the high-magnesium calcite of large foraminifera (26‰), while higher values (21-25‰) were measured on planktonic species (Holcomb et al., 2015; Hönisch et al., 2008; Rae et al., 2011; Sanyal et al., 1996). For gorgonian calcite corals, recent studies of the genus *Keratoisis* (bamboo coral) revealed low values of $\delta^{11}\text{B}$, between 14 and 17‰ (Farmer et al., 2015). Concerning inorganic calcite precipitated in the laboratory, Hemming et al. (1995) found no major $\delta^{11}\text{B}$ value difference between calcite and aragonite with values at about 16.5 ± 1.3 ‰ and Sanyal et al. (2000) calculated lower values, at around 19.25 ± 0.35 ‰ for inorganic calcite at seawater of pH range = 7.9-8.06. Nevertheless, more recent work showed that calcite and aragonite do not have the same fractionation factors with respect to boron isotopes (Noireaux et al., 2015). These authors suggest that this difference could be related to different pathways of boron incorporation in the calcite lattice compared to the aragonite one, such difference having also been shown by Uchikawa et al. (2015).

Low B/Ca ratios were observed in our “with-calcite” skeleton. Such ratios, equivalent to ~30 ppm of boron for the most calcite-rich samples (~30%) are clearly lower than values observed for modern *Porites* (Douville et al., 2010; Gaillardet and Allegre, 1995; Hemming and Hanson, 1992) but are similar to concentrations measured in some calcite benthic foraminifera (Rae et al., 2011; Yu et al., 2007; Yu et al., 2010) and in inorganic calcite (Gabitov et al., 2014).

Because the $\delta^{11}\text{B}$ decreases with the increase of the calcite-%, a decrease of the calculated pH_{sw} is observed with a rate of -0.011 ± 0.002 pH_{sw} per calcite-% (Fig. 6). Such impact is particularly pronounced and can strongly limit the use of $\delta^{11}\text{B}$ -pH proxy for corals, especially if the objective is to reconstruct the recent anthropogenic pH changes of the ocean. For illustration, 5% of calcite in *Porites* skeleton will decrease the reconstructed seawater pH by ~ 0.055 pH-unit whereas surface ocean acidification over the last two centuries due to industrial era for tropical areas is about 0.05-0.09 pH-unit (Pelejero et al., 2005; Sabine et al., 2004).

Recently, assumptions concerning the paleo-pH technique were revisited (Trotter et al., 2011), especially based on values of α of 1.026-1.027 for the theoretical factor of isotopic boron fractionation in seawater (Klochko et al., 2006; Nir et al., 2015). So Trotter et al. (2011) confirm previous studies (Allison et al., 2010; Blamart et al., 2007; Rollion-Bard et al., 2003) which made the assumption that the isotopic composition of boron in carbonate allows to calculate the pH of the calcifying solution ($\text{pH}_{\text{solution}}$) which is regulated by corals themselves during their calcification. In this assumption, a α value of 1.027 is used instead of 1.020 to determine $\text{pH}_{\text{solution}}$. Fortunately, such $\text{pH}_{\text{solution}}$ inferred from *Porites* would also depend on the seawater pH (pH_{sw}) following the *Porites*-specific formula: $\text{pH}_{\text{sw}} = (\text{pH}_{\text{solution}} - 5.954)/0.32$ (D'Olivo et al., 2015; McCulloch et al., 2012). By applying this approach, our new resulting pH_{sw} has low values (7.10-7.62), from 0.5 to 1 pH-unit lower than the mean regional seawater pH of 8.12 (Fig. 6). Again, a constant decrease in pH is observed with the increase of calcite-% (-0.014 ± 0.002 pH per calcite-%). Compared to the initial reconstructed seawater pH values (from the two first samples with calcite percentage lower than 2%), the relative pH change observed for 32% of calcite is of 5.4% (-0.43 pH-unit) by using Hönisch et al. (2007)'s approach and 6.7% (-0.51 pH-unit) using this last technique. This weak difference of relative pH change due to calcite presence, 6.7% against 5.4%, could be explained by the

difference in the calibration curves used but also by the difference of pH ranges reconstructed from the two methods (7.10-7.62 versus 7.53-7.96). Finally, independently of the pH-paleo techniques used, calcite-% needs to be lower than 1% for paleo-applications to limit the effect to ~ 0.01 pH-unit.

5. Conclusion

We analyzed a live-collected coral from a shallow setting in Vanuatu for a series of isotopes and element/Ca ratios, with a specific focus on SST (Sr/Ca, Li/Mg) and pH ($\delta^{11}\text{B}$) proxies. The colony presents two geochemical signatures related to the presence or absence of intra-skeletal calcite. The Sr/Ca variations due to the presence of intra-skeletal calcite occurrence are smaller than those previously reported, while no data were available so far for comparison for Li/Mg and $\delta^{11}\text{B}$. We conclude that i) SST reconstructions using Sr/Ca can only be done when less than 5% of intra-skeletal calcite is present, and temperature reconstructed from Li/Mg ratio appears more impacted by the calcite presence than Sr/Ca temperature; ii) qualitative data, e.g., seasonal amplitude changes, can be obtained using the Sr/Ca ratio changes even if 32% of intra-skeletal calcite is present; iii) the paleo-pH technique based on boron isotopes has to be applied on tropical corals, here a massive *Porites* species, free of calcite; and iv) assessment of the coral skeleton preservation, including calcite percentage and type, is necessary before interpreting any coral geochemical data, even those obtained on live-collected ones. We propose that the coral lived its last 5 years in a shallow setting that could have initiated a rainfall-related very early diagenesis but the process of calcite formation itself remains unknown.

Acknowledgments

Thanks to Louise Bordier for her contribution to trace element quantification using LSCE's ICP-QMS and to Paolo Montagna for his contribution to strontium stable isotope ratio acquisition. We thank C. Rollion-Bard, N. Allison, and an anonymous reviewer for their constructive comments. This is LSCE contribution n°XXXX. This work was funded by the national project MISTRALS/MERMEX/CALIBORON and by the ANR CARBORIC (Grant No. ANR-13-BS06-0013-04) of the French Agence Nationale de la Recherche. This paper is dedicated to our esteemed and dearly missed colleague Guy Cabioch. Without him, this work would not have been possible at all. This work was funded by the national project MISTRALS/MERMEX/CALIBORON.

References

- Alibert, C., Kinsley, L., Fallon, S.J., McCulloch, M.T., Berkelmans, R., McAllister, F. (2003) Source of trace element variability in Great Barrier Reef corals affected by the Burdekin flood plumes. *Geochim. Cosmochim. Acta* **67**, 231-246.
- Alibert, C., McCulloch, M.T. (1997) Strontium/calcium ratios in modern *Porites* corals from the Great Barrier Reef as a proxy for sea surface temperature: Calibration of the thermometer and monitoring of ENSO. *Paleoceanography* **12**, 345-363.
- Allison, N., Finch, A.A. (2004) High-resolution Sr/Ca records in modern *Porites lobata* corals: Effects of skeletal extension rate and architecture. *Geochem. Geophys. Geosyst.* **5**, Q05001, doi:05010.01029/02004GC000696.
- Allison, N., Finch, A.A., EIMF (2010) $\delta^{11}\text{B}$, Sr, Mg and B in a modern *Porites* coral: the relationship between calcification site pH and skeletal chemistry. *Geochim. Cosmochim. Acta* **74**, 1790-1800.

- Allison, N., Finch, A.A., Newville, M., Sutton, S.R. (2005a) Strontium in coral aragonite: 3. Sr coordination and geochemistry in relation to skeletal architecture. *Geochim. Cosmochim. Acta***69**, 3801-3811.
- Allison, N., Finch, A.A., Tudhope, A.W., Newville, M., Sutton, S.R., Ellam, R.M. (2005b) Reconstruction of deglacial sea surface temperatures in the tropical Pacific from selective analysis of a fossil coral - art. no. L17609. *Geophys. Res. Lett***32**, NIL_42-NIL_45.
- Allison, N., Finch, A.A., Webster, J.M., Clague, D.A. (2007) Palaeoenvironmental records from fossil corals: the effects of submarine diagenesis on temperature and climate estimates. *Geochim. Cosmochim. Acta***71**, 4693-4703.
- Ayling, B.F., McCulloch, M.T., Gagan, M.K., Stirling, C.H., Andersen, M.B., Blake, S.G. (2006) Sr/Ca and $\delta^{18}\text{O}$ seasonality in a *Porites* coral from the MIS 9 (339-303 ka) interglacial. *Earth and Planetary Science Letters***248**, 462-475.
- Bar-Matthews, M., Wasserburg, G.J., Chen, J.H. (1993) Diagenesis of fossil coral skeletons - correlation between trace-elements, textures, and U-234/U-238. *Geochim. Cosmochim. Acta***57**, 257-276.
- Beck, J.W., Edwards, R.L., Ito, E., Taylor, F.W., Recy, J., Rougerie, F., Joannot, P., Henin, C. (1992) Sea-surface temperature from coral skeletal strontium/calcium ratios. *Science***257**, 644-647.
- Benzerara, K., Menguy, N., Obst, M., Stolarski, J., Mazur, M., Tyliszczak, T., Brown Jr, G.E., Meibom, A. (2011) Study of the crystallographic architecture of corals at the nanoscale by scanning transmission X-ray microscopy and transmission electron microscopy. *Ultramicroscopy***111**, 1268-1275.
- Blamart, D., Rollion-Bard, C., Meibom, A., Cuif, J.-P., Juillet-Leclerc, A., Dauphin, Y. (2007) Correlation of boron isotopic composition with ultrastructure in the deep-sea coral

Lophelia pertusa: Implications for biomineralization and paleo-pH. *Geochemistry, Geophysics, Geosystems***8**, Q12001, doi:12010.11029/12007GC001686.

Bourdin, C., Douville, E., Genty, D. (2011) Alkaline-earth metal and rare-earth element incorporation control by ionic radius and growth rate on a stalagmite from the Chauvet Cave, Southeastern France. *Chem. Geol.***290**, 1-11.

Brahmi, C., Meibom, A., Smith, D.C., Stolarski, J., Auzoux-Bordenave, S., Nouet, J., Doumenc, D., Djediat, C., Domart-Coulon, I. (2010) Skeletal growth, ultrastructure and composition of the azooxanthellate scleractinian coral *Balanophyllia regia*. *Coral Reefs***29**, 175-189.

Bries, J., Debrot, A., Meyer, D. (2004) Damage to the leeward reefs of Curaçao and Bonaire, Netherlands Antilles from a rare storm event: Hurricane Lenny, November 1999. *Coral Reefs***23**, 297-307.

Case, D.H., Robinson, L.F., Auro, M.E., Gagnon, A.C. (2010) Environmental and biological controls on Mg and Li in deep-sea scleractinian corals. *Earth and Planetary Science Letters***300**, 215-225.

Cheal, A., Coleman, G., Delean, S., Miller, I., Osborne, K., Sweatman, H. (2002) Responses of coral and fish assemblages to a severe but short-lived tropical cyclone on the Great Barrier Reef, Australia. *Coral Reefs***21**, 131-142.

Clode, P.L., Lema, K., Saunders, M., Weiner, S. (2011) Skeletal mineralogy of newly settling *Acropora millepora* (Scleractinia) coral recruits. *Coral Reefs***30**, 1-8.

Clode, P.L., Marshall, A.T. (2002) Low temperature FESEM of the calcifying interface of a scleractinian coral. *Tissue and Cell***34**, 187-198.

Corrège, T. (2006) Sea surface temperature and salinity reconstruction from coral geochemical tracers. *Palaeogeogr. Palaeoclimatol. Palaeoecol.***232**, 408-428.

- Cuif, J.P., Dauphin, Y. (2005) The environment recording unit in coral skeletons: structural and chemical evidences of a biochemically driven stepping-growth process in coral fibres. *Biogeosciences***2**, 61-73.
- D'Olivo, J.P., McCulloch, M.T., Eggins, S.M., Trotter, J. (2015) Coral records of reef-water pH across the central Great Barrier Reef, Australia: assessing the influence of river runoff on inshore reefs. *Biogeosciences***12**, 1223-1236.
- Dalbeck, P., Cusack, M., Dobson, P.S., Allison, N., Fallick, A.E., Tudhope, A.W. (2011) Identification and composition of secondary meniscus calcite in fossil coral and the effect on predicted sea surface temperature. *Chem. Geol.***280**, 314-322.
- Dickson, A.G. (1990) Thermodynamics of the dissociation of boric-acid in potassium-chloride solutions from 273.15°K to 318.15°K. *Deep-Sea Research Part a-Oceanographic Research Papers***37**, 755-766.
- Dissard, D., Douville, E., Reynaud, S., Juillet-Leclerc, A., Montagna, P., Louvat, P., McCulloch, M. (2012) Light and temperature effects on $\delta^{11}\text{B}$ and B/Ca ratios of the zooxanthellate coral *Acropora* sp.: results from culturing experiments. *Biogeosciences***9**, 4589-4605.
- Douville, E., Paterné, M., Cabioch, G., Louvat, P., Gaillardet, J., Juillet-Leclerc, A., Ayliffe, L. (2010) Abrupt sea surface pH change at the end of the Younger Dryas in the central sub-equatorial Pacific inferred from boron isotope abundance in corals (Porites). *Biogeosciences***7**, 2445-2459.
- Fabricius, K.E., De'ath, G., Puotinen, M.L., Done, T., Cooper, T.F., Burgess, S.C. (2008) Disturbance gradients on inshore and offshore coral reefs caused by a severe tropical cyclone. *Limnol Oceanogr***53**, 690-704.
- Falini, G., Albeck, S., Weiner, S., Addadi, L. (1996) Control of aragonite or calcite polymorphism by mollusk shell macromolecules. *Science***271**, 67-69.

- Falini, G., Reggi, M., Fermani, S., Sparla, F., Goffredo, S., Dubinsky, Z., Levi, O., Dauphin, Y., Cuif, J.-P. (2013) Control of aragonite deposition in colonial corals by intra-skeletal macromolecules. *Journal of Structural Biology***183**, 226-238.
- Fallon, S.J., McCulloch, M.T., Alibert, C. (2003) Examining water temperature proxies in *Porites* corals from the Great Barrier Reef: a cross-shelf comparison. *Coral Reefs***22**, 389-404.
- Farmer, J.R., Hönisch, B., Robinson, L.F., Hill, T.M. (2015) Effects of seawater-pH and biomineralization on the boron isotopic composition of deep-sea bamboo corals. *Geochim. Cosmochim. Acta***155**, 86-106.
- Finch, A.A., Allison, N. (2003) Strontium in coral aragonite: 2. Sr coordination and the long-term stability of coral environmental records. *Geochim. Cosmochim. Acta***67**, 4519-4527.
- Foster, G.L., Pogge von Strandmann, P.A.E., Rae, J.W.B. (2010) Boron and magnesium isotopic composition of seawater. **11**, Q08015.
- Frankowiak, K., Mazur, M., Gothmann, A.M., Stolarski, J. (2013) Diagenetic alteration of Triassic coral from the aragonite Konservat-Lagerstätte in Alakir Çay, Turkey: implications for geochemical measurements. *Palaios***28**, 333-342.
- Gabitov, R.I., Rollion-Bard, C., Tripathi, A., Sadekov, A. (2014) In situ study of boron partitioning between calcite and fluid at different crystal growth rates. *Geochim. Cosmochim. Acta***137**, 81-92.
- Gagan, M.K., Ayliffe, L.K., Beck, J.W., Cole, J.E., Druffel, E.R.M., Dunbar, R.B., Schrag, D.P. (2000) New views of tropical paleoclimates from corals. *Quat. Sci. Rev.***19**, 45-64.
- Gagan, M.K., Ayliffe, L.K., Hopley, D., Cali, J.A., Mortimer, G.E., Chappell, J., McCulloch, M.T., Head, M.J. (1998) Temperature and Surface-Ocean Water Balance of the Mid-Holocene Tropical Western Pacific. *Science***279**, 1014-1018.

- Gaillardet, J., Allegre, C.J. (1995) Boron isotopic compositions of corals: Seawater or diagenesis record? *Earth and Planetary Science Letters***136**, 665-676.
- Gilmour, J.P., Smith, L.D. (2006) Category 5 cyclone at Scott Reef, northwestern Australia. *Coral Reefs***25**, 200-200.
- Goreau, T.F. (1959) The Physiology of Skeleton Formation in Corals. I. A Method for Measuring the Rate of Calcium Deposition by Corals under Different Conditions. *Biol. Bull.***116**, 59-75.
- Griffiths, N., Müller, W., Johnson, K.G., Aguilera, O.A. (2013) Evaluation of the effect of diagenetic cements on element/Ca ratios in aragonitic Early Miocene (~16 Ma) Caribbean corals: Implications for 'deep-time' palaeo-environmental reconstructions. *Palaeogeogr. Palaeoclimatol. Palaeoecol.***369**, 185-200.
- Gutjahr, M., Bordier, L., Douville, E., Farmer, J., Foster, G.L., Hathorne, E., Hönisch, B., Lemarchand, D., Louvat, P., McCulloch, M., Noireaux, J., Pallavicini, N., Rodushkin, I., Roux, P., Stewart, J., Thil, F., You, C.-F. (2014) Boron Isotope Intercomparison Project (BIIP): Development of a new carbonate standard for stable isotopic analyses. *Geophysical Research Abstracts***16**, EGU2014-5028-2011.
- Gvirtzman, G., Friedman, G.M., Miller, D.S. (1973) Control and distribution of uranium in coral reefs during diagenesis. *Journal of Sedimentary Research***43**, 985-997.
- Hathorne, E.C., Felis, T., Suzuki, A., Kawahata, H., Cabioch, G. (2013a) Lithium in the aragonite skeletons of massive Porites corals: A new tool to reconstruct tropical sea surface temperatures. *Paleoceanography***28**, 143-152.
- Hathorne, E.C., Gagnon, A., Felis, T., Adkins, J., Asami, R., Boer, W., Caillon, N., Case, D., Cobb, K.M., Douville, E., deMenocal, P., Eisenhauer, A., Garbe-Schönberg, C.D., Geibert, W., Goldstein, S., Hughen, K., Inoue, M., Kawahata, H., Kölling, M., Le Cornec, F., Linsley, B.K., McGregor, H.V., Montagna, P., Nurhati, I.S., Quinn, T.M.,

- Raddatz, J., Rebaubier, H., Robinson, L., Sadekov, A., Sherrell, R., Sinclair, D., Tudhope, A.W., Wei, G., Wong, H., Wu, H.C., You, C.-F. (2013b) Inter-laboratory study for coral Sr/Ca and other element/Ca ratio measurements. *Geochemistry, Geophysics, Geosystems***4**, 3730–3750.
- Hemming, N.G., Guilderson, T.P., Fairbanks, R.G. (1998) Seasonal variations in the boron isotopic composition of coral: A productivity signal? *Global Biogeochemical Cycles***12**, 581 (598GB02337)
- Hemming, N.G., Hanson, G.N. (1992) Boron isotopic composition and concentration in modern marine carbonates. *Geochim. Cosmochim. Acta***56**, 537-543.
- Hemming, N.G., Reeder, R.J., Hanson, G.N. (1995) Mineral-fluid partitioning and isotopic fractionation of boron in synthetic calcium carbonate. *Geochim. Cosmochim. Acta***59**, 371-379.
- Hendy, E.J., Gagan, M.K., Lough, J.M., McCulloch, M., deMenocal, P.B. (2007) Impact of skeletal dissolution and secondary aragonite on trace element and isotopic climate proxies in *Porites* corals. *Paleoceanography***22**, doi:10.1029/2007PA001462.
- Holcomb, M., DeCarlo, T.M., Schoepf, V., Dissard, D., Tanaka, K., McCulloch, M. (2015) Cleaning and pre-treatment procedures for biogenic and synthetic calcium carbonate powders for determination of elemental and boron isotopic compositions. *Chem. Geol.* <http://dx.doi.org/10.1016/j.chemgeo.2015.01.019>.
- Hönisch, B., Bickert, T., Hemming, N.G. (2008) Modern and Pleistocene boron isotope composition of the benthic foraminifer *Cibicides wuellerstorfi*. *Earth and Planetary Science Letters***272**, 309-318.
- Hönisch, B., Hemming, N.G. (2004) Ground-truthing the boron isotope-paleo-pH proxy in planktonic foraminifera shells: Partial dissolution and shell size effects. *Paleoceanography***19**.

- Hönisch, B., Hemming, N.G., Loose, B. (2007) Comment on "A critical evaluation of the boron isotope-pH proxy: The accuracy of ancient ocean pH estimates" by M. Pagani, D. Lemarchand, A. Spivack and J. Gaillardet. *Geochim. Cosmochim. Acta***71**, 1636-1641.
- Houk, J.E., Buddemeier, R.W., Chave, K.E. (1975) Skeletal Low-Magnesium Calcite in Living Scleractinian Corals. *Science***189**, 997-999.
- Inoue, M., Suwa, R., Suzuki, A., Sakai, K., Kawahata, H. (2011) Effects of seawater pH on growth and skeletal U/Ca ratios of *Acropora digitifera* coral polyps. *Geophys. Res. Lett.***38**, L12809.
- James, N.P. (1974) Diagenesis of scleractinian corals in the subaerial vadose environment. *Journal of Paleontology***48**, 785-799.
- Juillet-Leclerc, A., Reynaud, S., Dissard, D., Tisserand, G., Ferrier-Pagès, C. (2014) Light is an active contributor to the vital effects of coral skeleton proxies. *Geochim. Cosmochim. Acta***140**, 671-690.
- Klochko, K., Kaufman, A.J., Yao, W.S., Byrne, R.H., Tossell, J.A. (2006) Experimental measurement of boron isotope fractionation in seawater. *Earth and Planetary Science Letters***248**, 276-285.
- Krief, S., Hendy, E.J., Fine, M., Yam, R., Meibom, A., Foster, G.L., Shemesh, A. (2010) Physiological and isotopic responses of scleractinian corals to ocean acidification. *Geochim. Cosmochim. Acta***74**, 4988-5001.
- Lazareth, C.E., Bustamante Rosell, M.G., Turcq, B., Le Cornec, F., Mandeng-Yogo, M., Caquineau, S., Cabioch, G. (2013) Mid-Holocene climate in New Caledonia (southwest Pacific): coral and PMIP models monthly resolved results. *Quat. Sci. Rev.***69**, 83-97.
- Lécuyer, C., Grandjean, P., Reynard, B., Albarède, F., Telouk, P. (2002) $^{11}\text{B}/^{10}\text{B}$ analysis of geological materials by ICP-MS Plasma 54: Application to the boron fractionation between brachiopod calcite and seawater. *Chem. Geol.***186**, 45-55.

- Liu, Y., Liu, W., Peng, Z., Xiao, Y., Wei, G., Sun, W., He, J., Liu, G., Chou, C.-L. (2009) Instability of seawater pH in the South China Sea during the mid-late Holocene: Evidence from boron isotopic composition of corals. *Geochim. Cosmochim. Acta***73**, 1264-1272.
- Longman, M.W. (1980) Carbonate diagenetic textures from nearsurface diagenetic environments. *Am. Assoc. Petrol. Geol. Bulletin***64**, 461-487.
- Marubini, F., Barnett, H., Langdon, C., Atkinson, M.J. (2001) Dependence of calcification on light and carbonate ion concentration for the hermatypic coral *Porites compressa*. *Marine Ecology-Progress Series***220**, 153-162.
- Mass, T., Drake, Jeana L., Haramaty, L., Kim, J.D., Zelzion, E., Bhattacharya, D., Falkowski, Paul G. (2013) Cloning and Characterization of Four Novel Coral Acid-Rich Proteins that Precipitate Carbonates In Vitro. *Current Biology***23**, 1126-1131.
- McCulloch, M., Trotter, J., Montagna, P., Falter, J., Dunbar, R., Freiwald, A., Försterra, G., López Correa, M., Maier, C., Rüggeberg, A., Taviani, M. (2012) Resilience of cold-water scleractinian corals to ocean acidification: Boron isotopic systematics of pH and saturation state up-regulation. *Geochim. Cosmochim. Acta***87**, 21-34.
- McGregor, H.V., Gagan, M.K. (2003) Diagenesis and geochemistry of *Porites* corals from Papua New Guinea: Implications for paleoclimate reconstruction. *Geochim. Cosmochim. Acta***67**, 2147-2156.
- Meibom, A., Mostefaoui, S., Cuif, J.-P., Dauphin, Y., Houlbreque, F., Dunbar, R., Constantz, B. (2007) Biological forcing controls the chemistry of reef-building coral skeleton. *Geophys. Res. Lett.***34**, L02601.
- Montagna, P., McCulloch, M., Douville, E., López Correa, M., Trotter, J., Rodolfo-Metalpa, R., Dissard, D., Ferrier-Pagès, C., Frank, N., Freiwald, A., Goldstein, S., Mazzoli, C., Reynaud, S., Rüggeberg, A., Russo, S., Taviani, M. (2014) Li/Mg systematics in

- scleractinian corals: Calibration of the thermometer. *Geochim. Cosmochim. Acta***132**, 288-310.
- Moreau, M., Corrège, T., Dassié, E.P., Le Cornec, F. (2015) Evidence for the non-influence of salinity variability on the *Porites* coral Sr/Ca palaeothermometer. *Clim. Past***11**, 523-532.
- Nir, O., Vengosh, A., Harkness, J.S., Dwyer, G.S., Lahav, O. (2015) Direct measurement of the boron isotope fractionation factor: Reducing the uncertainty in reconstructing ocean paleo-pH. *Earth and Planetary Science Letters***414**, 1-5.
- Noireaux, J., Mavromatis, V., Gaillardet, J., Schott, J., Montouillout, V., Louvat, P., Rollion-Bard, C., Neuville, D.R. (2015) Crystallographic control on the boron isotope paleo-pH proxy. *Earth and Planetary Science Letters***430**, 398-407.
- Nothdurft, L.D., Webb, G.E. (2007) Microstructure of common reef-building coral genera *Acropora*, *Pocillopora*, *Goniastrea* and *Porites*: constraints on spatial resolution in geochemical sampling. *Facies***53**, 1-26.
- Nothdurft, L.D., Webb, G.E. (2009) Earliest diagenesis in scleractinian coral skeletons: implications for palaeoclimate-sensitive geochemical archives. *Facies***55**, 161-201.
- Paillard, D., Labeyrie, L., Yiou, P. (1996) Macintosh Program performs time-series analysis. *Eos, Transactions American Geophysical Union***77**, 379-379.
- Palmiotto, C., Corda, L., Ligi, M., Cipriani, A., Dick, H.J.B., Douville, E., Gasperini, L., Montagna, P., Thil, F., Borsetti, A.M., Balestra, B., Bonatti, E. (2013) Nonvolcanic tectonic islands in ancient and modern oceans. *Geochemistry, Geophysics, Geosystems***14**, 4698-4717.
- Pelejero, C., Calvo, E., McCulloch, M.T., Marshall, J.F., Gagan, M.K., Lough, J.M., Opdyke, B.N. (2005) Preindustrial to modern interdecadal variability in coral reef pH. *Science***309**, 2204-2207.

- Penman, D.E., Hönisch, B., Rasbury, E.T., Hemming, N.G., Spero, H.J. (2013) Boron, carbon, and oxygen isotopic composition of brachiopod shells: Intra-shell variability, controls, and potential as a paleo-pH recorder. *Chem. Geol.***340**, 32-39.
- Perrin, C. (2003) Compositional heterogeneity and microstructural diversity of coral skeletons: implications for taxonomy and control on early diagenesis. *Coral Reefs***22**, 109-120.
- Perrin, C., Smith, D.C. (2007a) Decay of skeletal organic matrices and early diagenesis in coral skeletons. *Comptes Rendus Palevol***6**, 253-260.
- Perrin, C., Smith, D.C. (2007b) Earliest steps of diagenesis in living scleractinian corals: Evidence from ultrastructural pattern and raman spectroscopy. *Journal of Sedimentary Research***77**, 495-507.
- Pingitore, N.E. (1976) Vadose and phreatic diagenesis; processes, products and their recognition in corals. *Journal of Sedimentary Research***46**, 985-1006.
- Puverel, S., Tambutté, E., Zoccola, D., Domart-Coulon, I., Bouchot, A., Lotto, S., Allemand, D., Tambutté, S. (2005) Antibodies against the organic matrix in scleractinians: a new tool to study coral biomineralization. *Coral Reefs***24**, 149-156.
- Rabier, C., Anguy, Y., Cabioch, G., Genthon, P. (2008) Characterization of various stages of calcitization in *Porites sp* corals from uplifted reefs – Case studies from New-Caledonia, Vanuatu, and Futuna (South-West Pacific). *Sedimentary Geology***211**, 73-86.
- Rae, J.W.B., Foster, G.L., Schmidt, D.N., Elliott, T. (2011) Boron isotopes and B/Ca in benthic foraminifera: Proxies for the deep ocean carbonate system. *Earth and Planetary Science Letters***302**, 403-413.
- Rahman, M.A., Oomori, T., Wörheide, G. (2011) Calcite formation in soft coral sclerites is determined by a single reactive extracellular protein. *Journal of Biological Chemistry***286**, 31638-31649.

- Reynaud, S., Hemming, N.G., Juillet-Leclerc, A., Gattuso, J.-P. (2004) Effect of pCO₂ and temperature on the boron isotopic composition of the zooxanthellate coral *Acropora* sp. *Coral Reefs* **23**, 539-546.
- Reynolds, R.W., Rayner, N.A., Smith, T.M., Stokes, D.C., Wang, W. (2002) An improved *in situ* and satellite SST analysis for climate. *Journal of Climate* **15**, 1609-1625.
- Rollion-Bard, C., Chaussidon, M., France-Lanord, C. (2003) pH control on oxygen isotopic composition of symbiotic corals. *Earth and Planetary Science Letters* **215**, 275-288.
- Sabine, C.L., Feely, R.A., Gruber, N., Key, R.M., Lee, K., Bullister, J.L., Wanninkhof, R., Wong, C.S., Wallace, D.W.R., Tilbrook, B., Millero, F.J., Peng, T.-H., Kozyr, A., Ono, T., Rios, A.F. (2004) The oceanic sink for anthropogenic CO₂. *Science* **305**, 367-371.
- Sanyal, A., Hemming, N.G., Broecker, W.S., Lea, D.W., Spero, H.J., Hanson, G.N. (1996) Oceanic pH control on the boron isotopic composition of foraminifera: Evidence from culture experiments. *Paleoceanography* **11**, 513-517.
- Sanyal, A., Nugent, M., Reeder, R.J., Bijma, J. (2000) Seawater pH control on the boron isotopic composition of calcite: evidence from inorganic calcite precipitation experiments. *Geochim. Cosmochim. Acta* **64**, 1551-1555.
- Shinjo, R., Asami, R., Huang, K.-F., You, C.-F., Iryu, Y. (2013a) Ocean acidification trend in the tropical North Pacific since the mid-20th century reconstructed from a coral archive. *Marine Geology* **342**, 58-64.
- Shinjo, R., Asami, R., Huang, K.-F., You, C.-F., Iryu, Y. (2013b) Ocean acidification trend in the tropical North Pacific since the mid-20th century reconstructed from a coral archive. *Mar. Geol.* **342**, 58-64.
- Sinclair, D.J., McCulloch, M.T. (2004) Corals record low mobile barium concentrations in the Burdekin River during the 1974 flood: evidence for limited Ba supply to rivers? *Palaeogeogr. Palaeoclimatol. Palaeoecol.* **214**, 155-174.

- Sinclair, D.J., Williams, B., Allard, G., Ghaleb, B., Fallon, S., Ross, S.W., Risk, M. (2011) Reproducibility of trace element profiles in a specimen of the deep-water bamboo coral *Keratoisis* sp. *Geochim. Cosmochim. Acta***75**, 5101-5121.
- Sorauf, J.E. (1980) Biomineralization. structure and diagenesis of the coelenterate skeleton. *Acta Palaeontologica Polonica***25**, 327-343.
- Stolarski, J., Mazur, M. (2005) Nanostructure of biogenic versus abiogenic calcium carbonate crystals. *Acta Palaeontologica Polonica***50**, 847-865.
- Sun, D., Su, R., McConnaughey, T.A., Bloemendal, J. (2008) Variability of skeletal growth and $\delta^{13}\text{C}$ in massive corals from the South China Sea: Effects of photosynthesis, respiration and human activities. *Chem. Geol.***255**.
- Tambutté, E., Allemand, D., Zoccola, D., Meibom, A., Lotto, S., Caminiti, N., Tambutté, S. (2007) Observations of the tissue-skeleton interface in the scleractinian coral *Stylophora pistillata*. *Coral Reefs***26**, 517-529.
- Tambutté, S., Holcomb, M., Ferrier-Pagès, C., Reynaud, S., Tambutté, É., Zoccola, D., Allemand, D. (2011) Coral biomineralization: From the gene to the environment. *J. Exp. Mar. Biol. Ecol.***408**, 58-78.
- Thresher, R.E., Wilson, N.C., MacRae, C.M., Neil, H. (2010) Temperature effects on the calcite skeletal composition of deep-water gorgonians (Isididae). *Geochim. Cosmochim. Acta***74**, 4655-4670.
- Trotter, J., Montagna, P., McCulloch, M., Silenzi, S., Reynaud, S., Mortimer, G., Martin, S., Ferrier-Pagès, C., Gattuso, J.-P., Rodolfo-Metalpa, R. (2011) Quantifying the pH 'vital effect' in the temperate zooxanthellate coral *Cladocora caespitosa*: Validation of the boron seawater pH proxy. *Earth and Planetary Science Letters* 10.1016/j.epsl.2011.01.030.

- Uchikawa, J., Penman, D.E., Zachos, J.C., Zeebe, R.E. (2015) Experimental evidence for kinetic effects on B/Ca in synthetic calcite: Implications for potential B(OH)₄⁻ and B(OH)₃ incorporation. *Geochim. Cosmochim. Acta***150**, 171-191.
- Venn, A., Tambutté, E., Holcomb, M., Allemand, D., Tambutté, S. (2011) Live tissue imaging shows reef corals elevate pH under their calcifying tissue relative to seawater. *PLoS One***6**, e20013, doi:20010.21371/journal.pone.0020013.
- Wei, G., McCulloch, M.T., Mortimer, G., Deng, W., Xie, L. (2009) Evidence for ocean acidification in the Great Barrier Reef of Australia. *Geochim. Cosmochim. Acta***73**, 2332-2346.
- Wei, G., Sun, M., Li, X., Nie, B. (2000) Mg/Ca, Sr/Ca and U/Ca ratios of a porites coral from Sanya Bay, Hainan Island, South China Sea and their relationships to sea surface temperature. *Palaeogeogr. Palaeoclimatol. Palaeoecol.***162**, 59-74.
- Wu, H.C., Linsley, B.K., Dassié, E.P., Schiraldi, B., deMenocal, P.B. (2013) Oceanographic variability in the South Pacific Convergence Zone region over the last 210 years from multi-site coral Sr/Ca records. *Geochemistry, Geophysics, Geosystems***14**, 1435-1453.
- Yu, J., Elderfield, H., Hönisch, B. (2007) B/Ca in planktonic foraminifera as a proxy for surface seawater pH. *Paleoceanography***22**, PA2202, doi:2210.1029/2006PA001347.
- Yu, J., Foster, G.L., Elderfield, H., Broecker, W.S., Clark, E. (2010) An evaluation of benthic foraminiferal B/Ca and $\delta^{11}\text{B}$ for deep ocean carbonate ion and pH reconstructions. *Earth and Planetary Science Letters***293**, 114-120.
- Zinke, J., Pfeiffer, M., Park, W., Schneider, B., Reuning, L., Dullo, W.C., Camoin, G.F., Mangini, A., Schroeder-Ritzrau, A., Garbe-Schoenberg, D., Davies, G.R. (2014) Seychelles coral record of changes in sea surface temperature bimodality in the western Indian Ocean from the Mid-Holocene to the present. *Climate Dynamics***43**, 689-708.

Figure captions

Figure 1: Location of the sampling site. (A) Location of Vanuatu in the West Pacific and of the Epi Island (square B), (B) Location of the Mapuna Bay on the Epi Island, where the coral colony was collected.

Figure 2: X-ray picture of the *Porites sp.* colony studied with location of the geochemical samples and of the XRD analyses. The black arrow points the trace left by the sampling procedure for trace element profile. To the right of this profile, the rectangles represent the coral parts sampled at approximately yearly scale ($\delta^{11}\text{B}$, trace element and XRD). The white numbers are the calcite percentages (from XRD analyses) with associated uncertainties specified below (*italic*). "tr." stands for "trace". The growth direction change, most probably related to the Ivy cyclone (2004), is underlined by the dotted bold line.

Figure 3: Microstructure features of the "no-calcite" coral skeleton (SEM pictures). Arrows point microborer galleries. (A) Overview of the coral skeleton showing the well-preserved skeleton, (B) Enlargement of a transversal cut of a septum. The aragonite fibers are very well preserved, i.e., without any dissolution features. The microborer galleries are empty, i.e., without any secondary mineral precipitation, (C) Higher magnification on the microborer galleries transversally cut, (D) Enlargement of the center of calcification (COC) from image "C" showing the well-preserved microgranular and fibrous structure of aragonite crystals.

Figure 4: Microstructure features of the "with-calcite" coral skeleton (SEM pictures). (A) Overview of the coral skeleton. No secondary precipitation is observed in the inter-skeletal pore spaces, (B) Calcite filling microborer galleries, (C) Enlargement of a septum. The

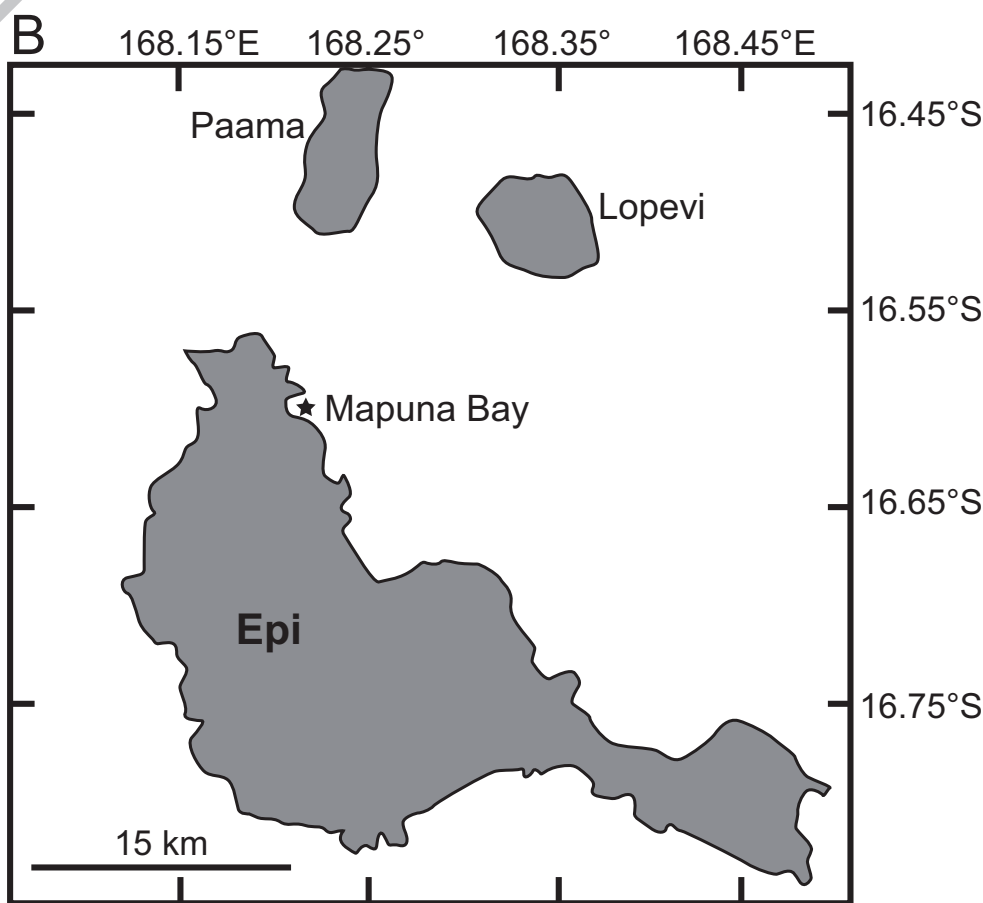
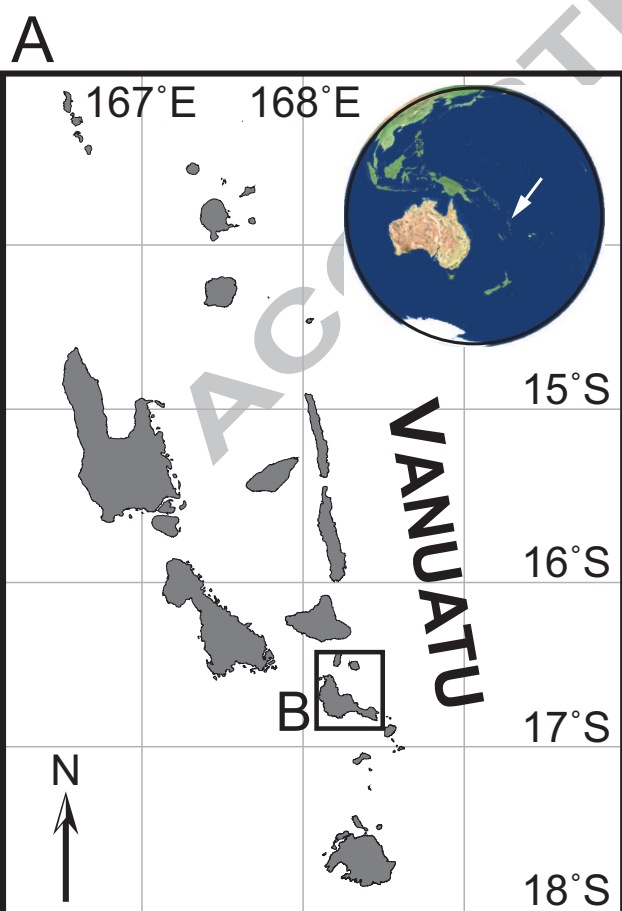
aragonite fibers are very well preserved, i.e., without any dissolution features. Patches of calcite occur along the center of calcification (COC) line (black arrows + c), (D-E) Enlargement of calcite replacing COC completely. The aragonite fibers are well preserved (no dissolution) and the contact between the calcite and the aragonite fibers is neat, (F-H) Enlargement of calcite partly replacing COCs. The aragonite fibers are well preserved (no dissolution) and the contact between the calcite and the aragonite fibers is either neat (G) or calcite is separated from the aragonite fibers by granular aragonite characteristic of COC (H). Abbreviations: "c" = calcite; "a" = aragonite, "ga" = granular aragonite. White arrows point microborer galleries.

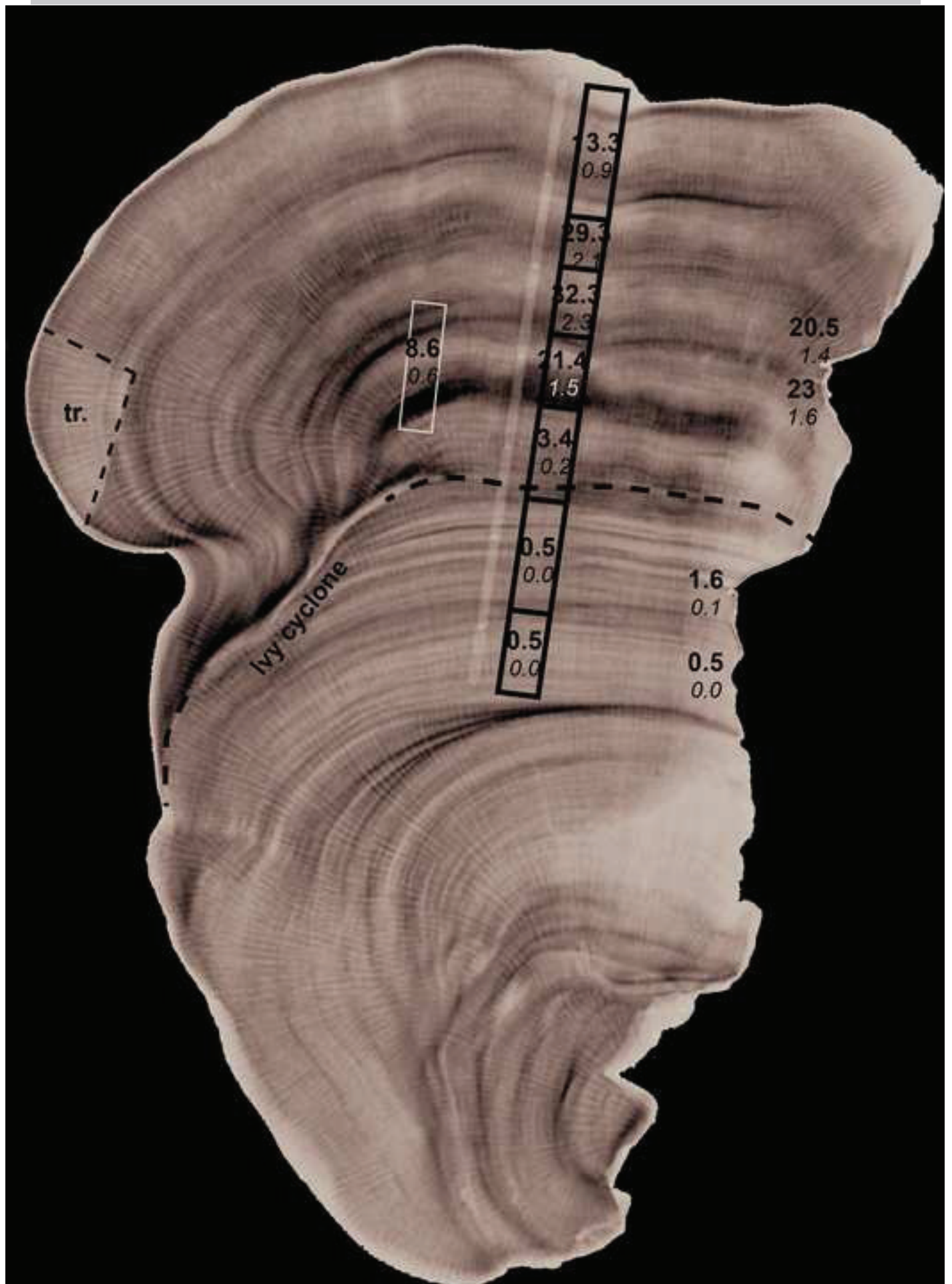
Figure 5: Geochemical record obtained from the Vanuatu Epi colony. The numbers are the mean ± 1 SD (from the seasonal data) of the element/Ca ratio considered for the "no-calcite" and the "with-calcite" skeleton. The grey squares represent the yearly data. The 1σ precision on the element/Ca ratio is shown for the seasonal data. When not visible, this error is smaller than the symbol. The grey area underlines the "with-calcite" part of the skeleton. The grey line materialized the date when the Ivy Cyclone passed above Vanuatu. (A) Sr/Ca. The star represents the 2007-08 La Niña event, (B) U/Ca, (C) Mg/Ca, (D) Li/Mg, (E) B/Ca at the monthly resolution (black squares) and B/Ca and $\delta^{11}\text{B}$ at the yearly resolution (grey squares and white circles respectively). For (E), numbers are B/Ca mean ± 1 SD from the high-resolution B/Ca profile.

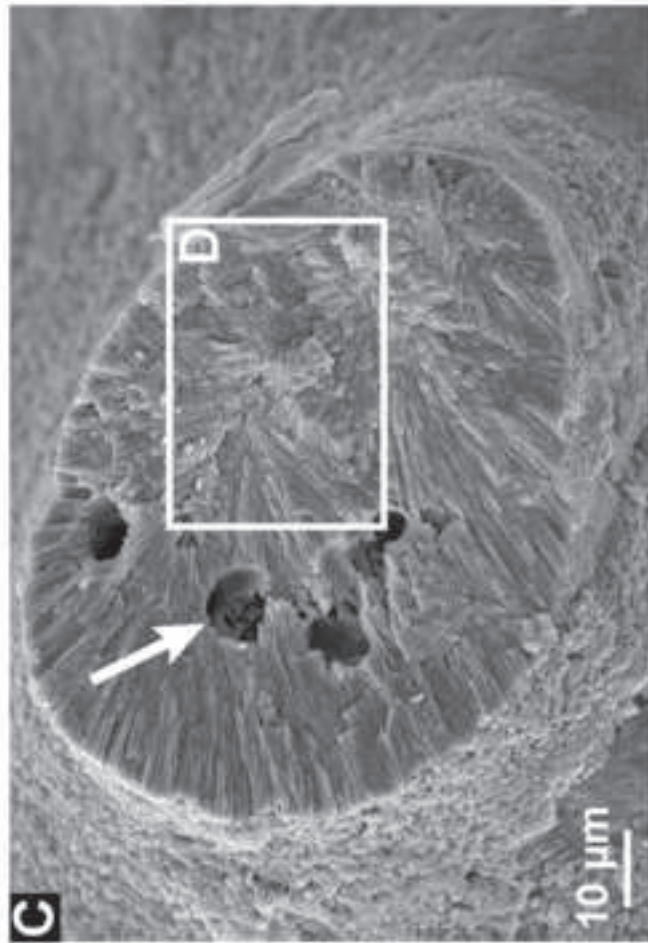
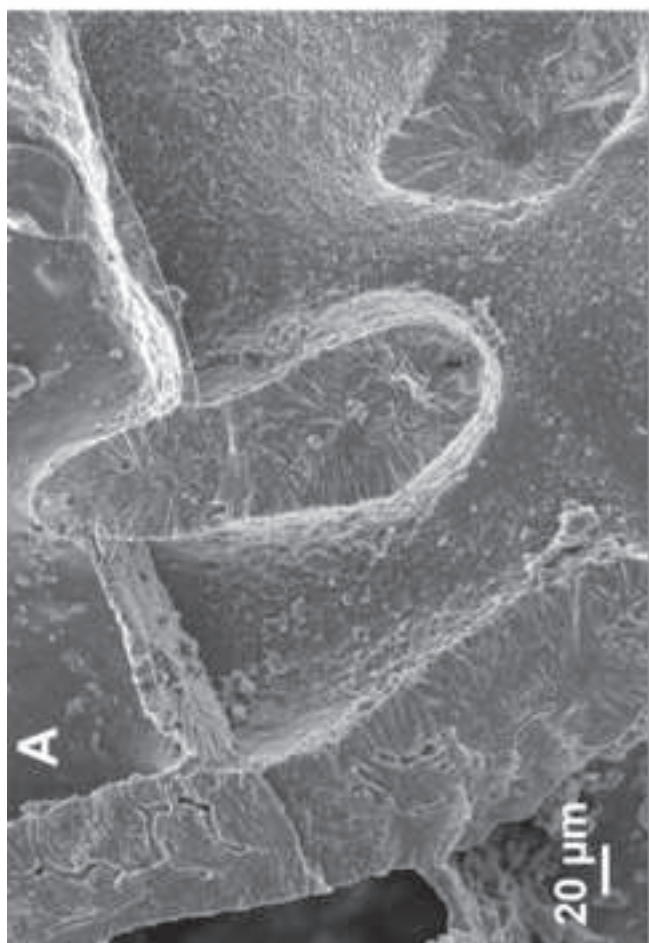
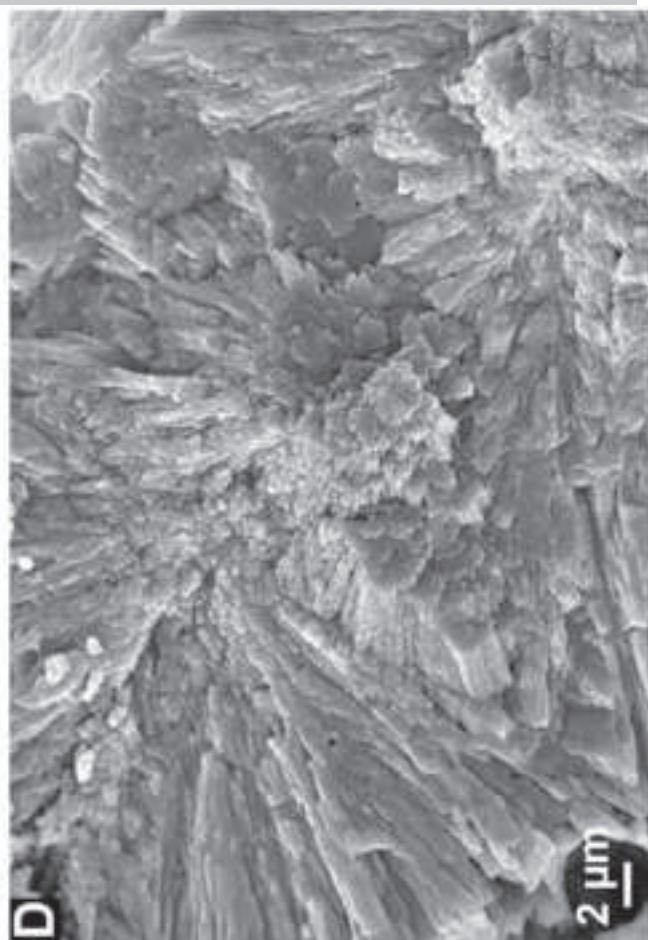
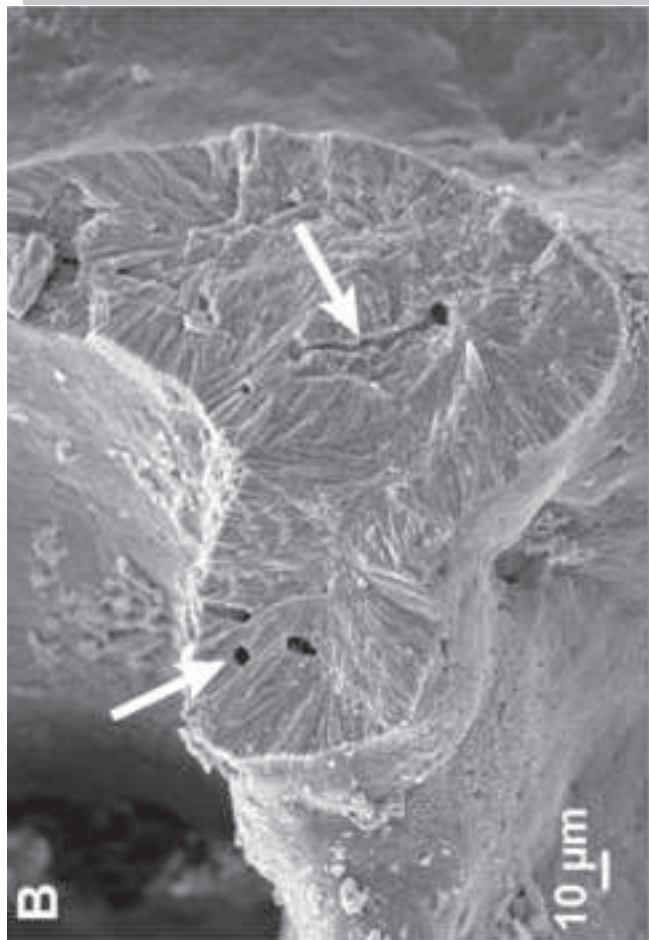
Figure 6: Influence of intra-skeletal calcite on the $\delta^{11}\text{B}$ signature and on reconstructed seawater pH (pH_{sw}). The parameters for calculation of pH_{sw} are: $\alpha = 1.020$ (Hönisch et al., 2007); $\delta^{11}\text{B}_{\text{seawater}} = 39.61\text{‰}$ (Foster et al., 2010); $\text{pK}_{\text{B}} = 8.56$ (Dickson, 1990) corresponding to average temperature and salinity values of 27.9°C and 34.88, respectively. The horizontal

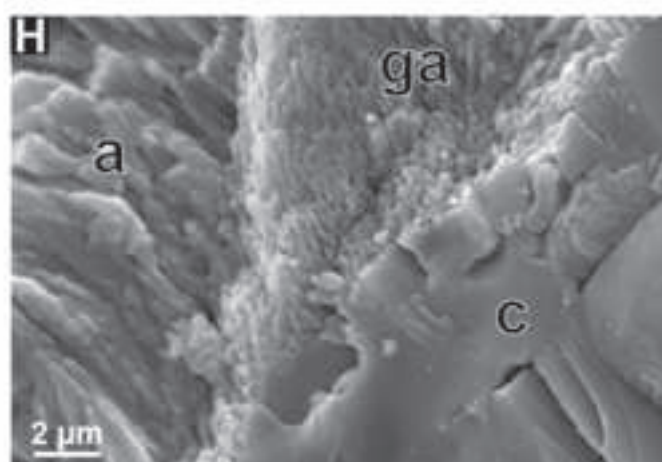
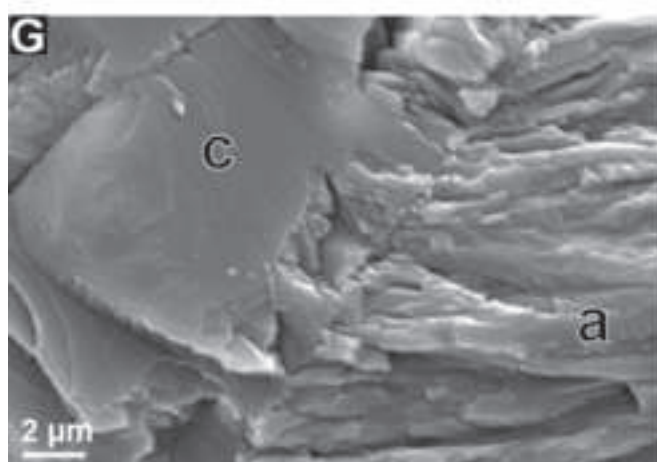
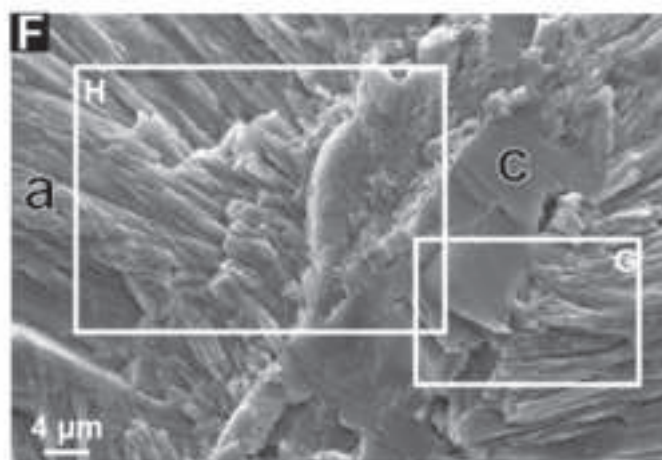
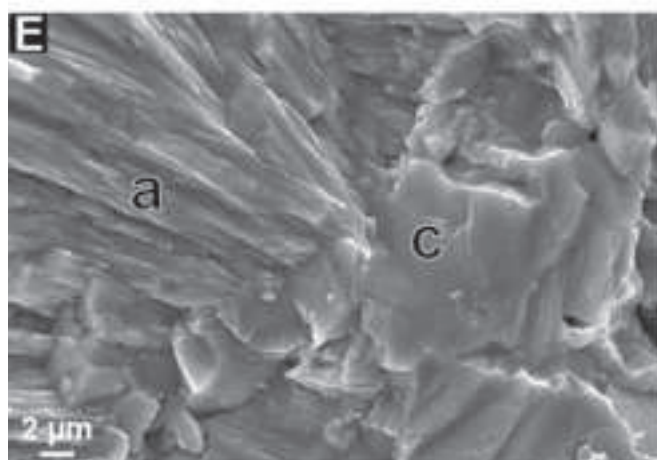
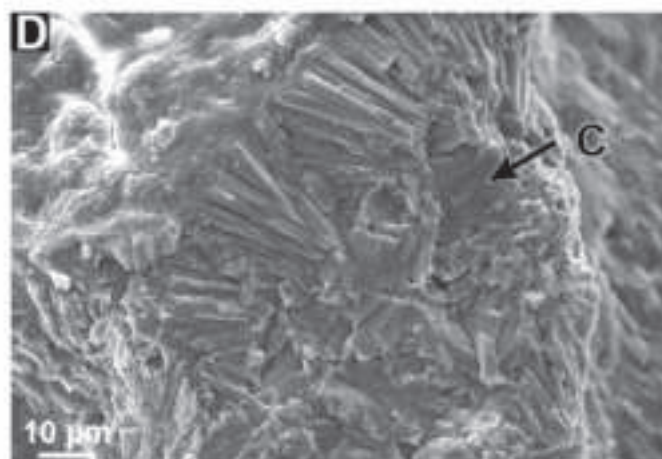
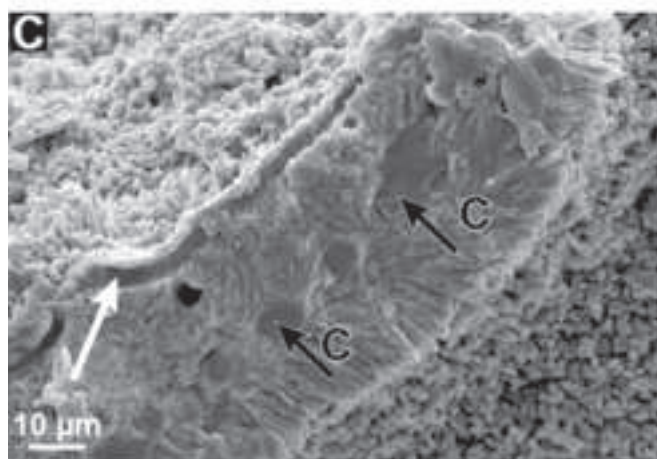
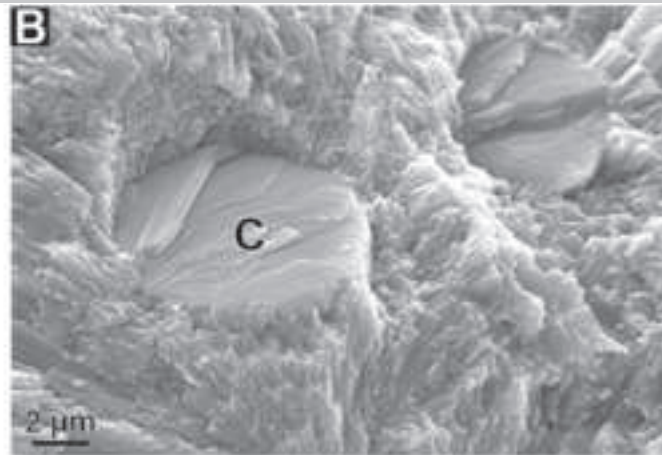
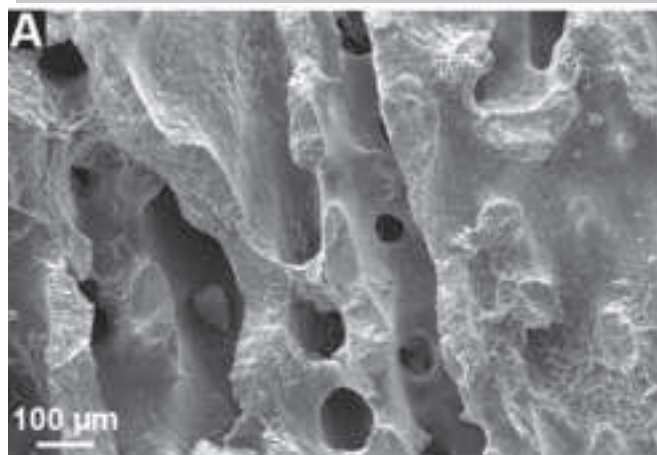
grey bar represents the mean regional seawater pH (8.12 ± 0.02) from the marine carbon cycle database PACIFICA (referenced cruise 49NZ20090521; 318MWESTW_5; 35A319940923; area: 12-20°S / 164-170 W; n= 37 for the shallow layer 0-50 m). Linear regression lines, uncertainties and r^2 are shown, as well as the related equations for $\delta^{11}\text{B}$ and pH_{sw} vs. calcite-%.

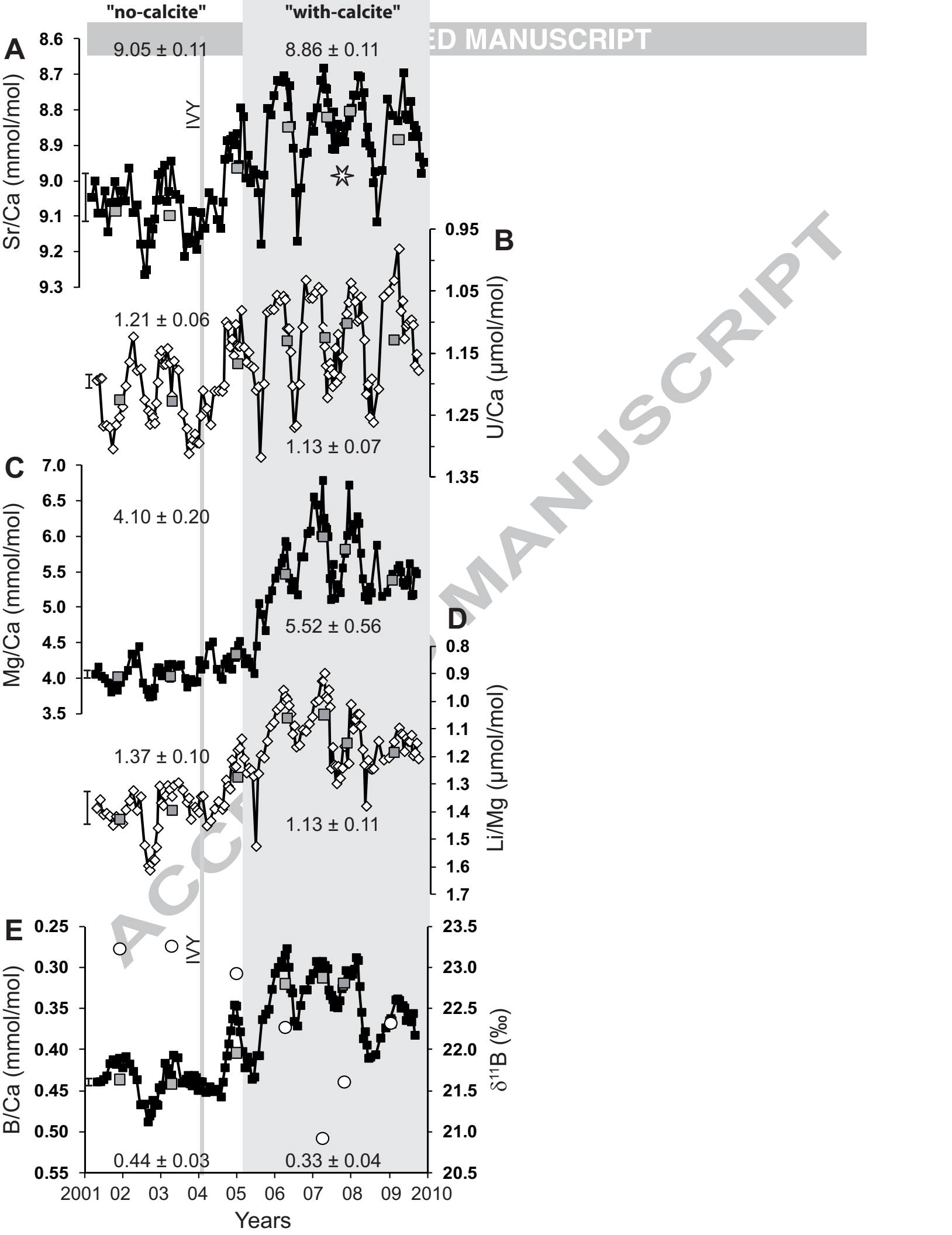
Figure 7: Comparison between reconstructed and gridded SST. Reconstructed SSTs were calculated from the Sr/Ca and Li/Mg profiles. Gridded SST was obtained for a box centered on 168.5E-16.5S (IGOSS, Reynold and Smith 02). Grey area: "with-calcite" skeleton part (see text for details). (A) Time series for the reconstructed (lines with symbols) and the gridded SST (grey line). The star represents the 2007-08 La Niña event, (B) Comparison of mean SST data for gridded vs. calculated SST (mean \pm Bonferroni confidence interval at 95%).

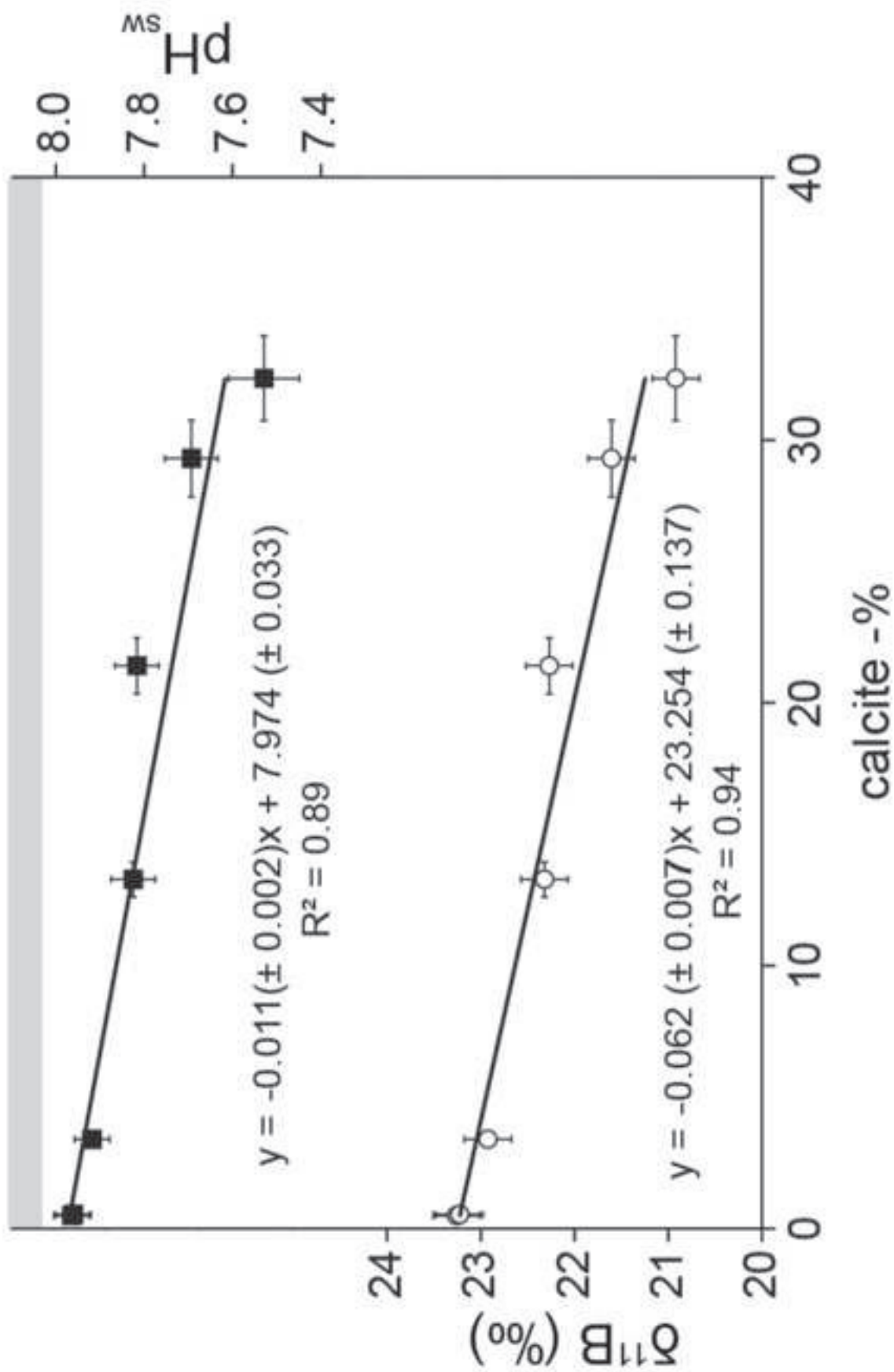












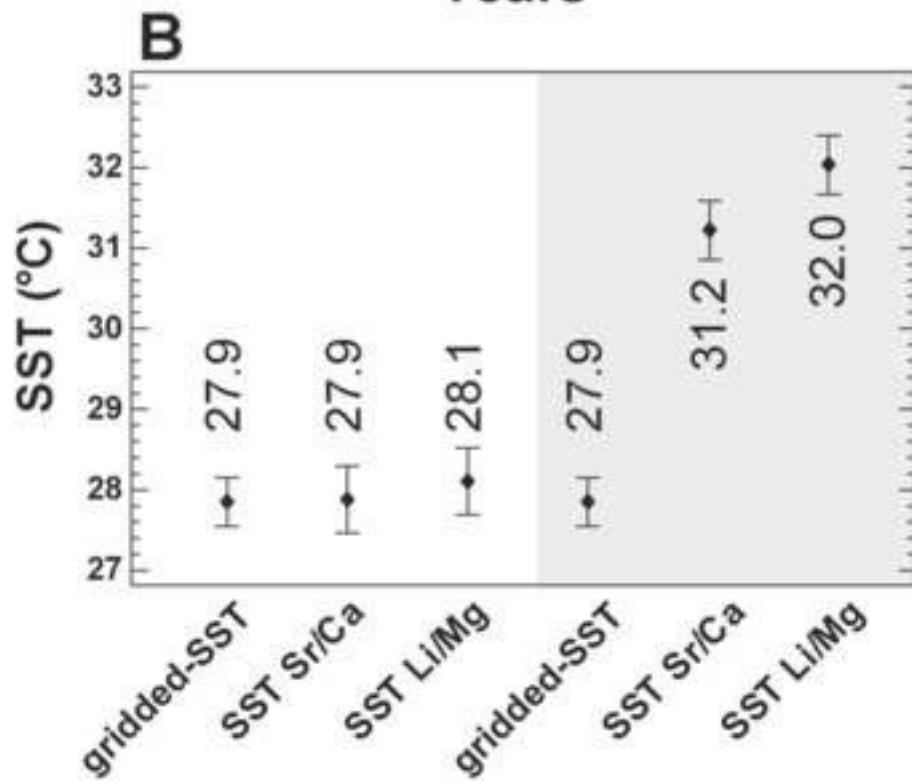
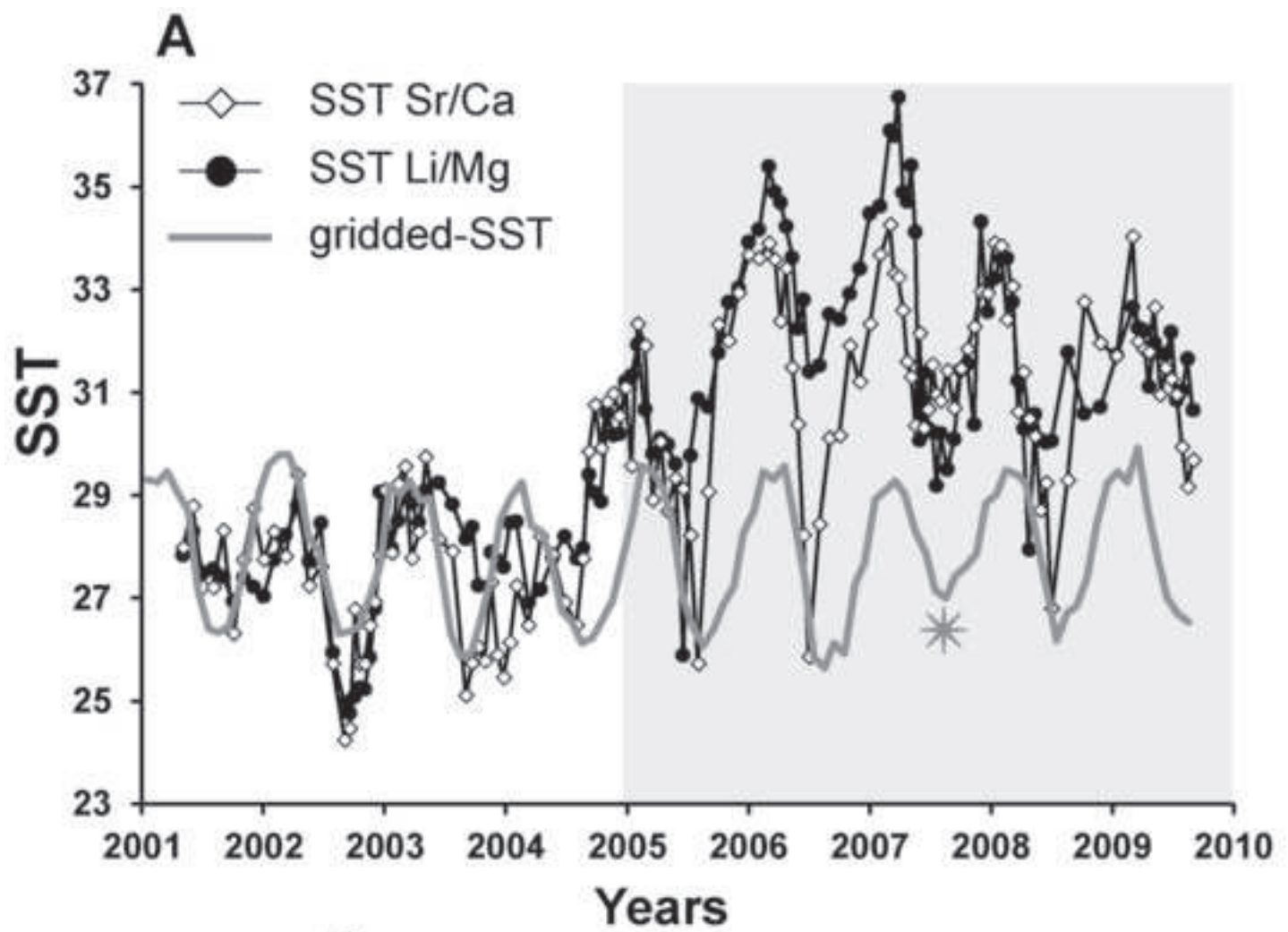


Table 1: Impact of the presence of calcite on coral skeleton geochemistry with an emphasis on Sr/Ca ratio changes and its related impact on sea surface temperature reconstructions ($^{\circ}\text{C}$ per 1% calc. = impact on SST values in $^{\circ}\text{C}$ per 1% of calcite in the coral skeleton). Unless specified, coral studied are *Porites sp.* (table not exhaustive). Data are presented in alphabetic order of first author. The nature of the calcite is reported. Cement means calcite present in the pores of the skeleton. Dissol.: dissolution of the skeleton. The effect on the geochemical signature is indicated by upward and downward arrows for "increasing" and "decreasing" element/Ca ratio content. The methodology used is specified with "specific" that means methodology allowing to analyze calcite solely (e.g., electron microprobe) and "bulk" methodology where whole parts of skeleton was analysed, i.e., a mixture of aragonite and calcite. The % calcite presents in the bulk analyze is specified (when applicable). The species in Griffiths et al. (2013) are *Siderastrea conferta* and *Montastraea limbata*. For Sayani et al. (2011), the $^{\circ}\text{C}$ per 1% calc. was calculated based on their maximal % of calcite (30%) for a maximal impact of $+11^{\circ}\text{C}$. For Frankowiak et al. (2013); the $^{\circ}\text{C}$ per %-calc. was calculated based on their $+3.3^{\circ}\text{C}$ for 13.8% of calcite. For this study, the $^{\circ}\text{C}$ per 1% calc. was calculated based on our $\sim +3.35^{\circ}\text{C}$ for 24% calcite. *: Sr/Ca mean value was evaluated based on the fig. 8 of Rabier et al. (2008). **: In this case, "bulk" is similar to "specific" because samples were highly (or totally) calcitised, i.e., only calcite portion of the coral is considered here.

<i>Coral</i>	<i>Calcite</i>	<i>Effect on element/Ca ratios</i>	<i>Method</i>	<i>Sr/Ca calcite (mmol/mol)</i>	<i>$^{\circ}\text{C}$ per 1% calc.</i>	<i>Reference</i>
Fossil	Cement	Sr \searrow , Mg \nearrow , B \searrow , U \nearrow	specific	1.51 ± 0.5 ; 0.99 ± 0.24	$\sim +1^{\circ}\text{C}$	Allison et al., 2007
Fossil	Dissepiment replacement	Sr \searrow	specific	2.93 ± 2.1	$\sim +1.2^{\circ}\text{C}$	Dalbeck et al., 2011
Fossil, <i>Pachysolemia cylindrica</i>	in COC, fibers, cement	Sr \nearrow , Mg \nearrow	bulk	7.69 for 13.8% calcite	$\sim -0.24^{\circ}\text{C}$	Frankowiak et al., 2013
Fossil, <i>S. conferta</i> & <i>M. limbata</i>	Cement	Sr \searrow , Mg \nearrow , B \searrow , Ba \searrow , U =	specific	0.41 ± 0.03	$+1.7^{\circ}\text{C}$	Griffiths et al., 2013
Live	Intra-skeletal	Sr \searrow , Mg \nearrow	bulk	3 for 100% calcite (extrapolated)	/	Houk et al. (1975)

Fossil	Cement & intra-skeletal	Sr ↓	bulk	8 to 2.1	~ + 1.15°C	McGregor and Gagan, 2003
Live	Filling microboring	Sr ↓, Mg ↑	specific	6.3 ± 1.0	/	Nothdurft et al., 2007
Fossil	Cement & intra-skeletal	Sr ↓, Mg ↑	specific	1.74: cement 7.7*: intra-squelette	/	Rabier et al., 2008
750 yr-old	Cement + dissol.	Sr ↓	specific	1.96 to 9.74	~ + 0.4°C	Sayani et al., 2011
Fossil	Intra-skeletal	Sr ↓, Ba ↓, U ↓, Mn ↑	bulk	3.43 ± 0.36 (~ 100% calcite)	/	Webb et al., 2009**
Live	In COC	Sr ↓, Mg ↑, U ↓, Li ↓, B ↓, δ ¹¹ B ↑, Ba =	bulk	8.84 for 24% calcite 7.96 ± 0.31 (~ 100% calcite)	~ + 0.13°C	This study